Doctoral Dissertation

Study on Synthesis and Properties of Thermo-Responsive Lamellar Hydrogels

(熱応答性層状ハイドロゲルの合成と特性に関する研究)

By

Yang HAN

Supervisor: Jian Ping GONG

Tasuku NAKAJIMA

Laboratory of Soft & Wet Matter,

Graduate School of Life Science, Hokkaido University

Sapporo 001-0021, Japan

March, 2024

Contents

List of important abbreviations

DGI	*n*-$C_{12}H_{25}$-$OCOCH_2C$-(=CH_2)$COOCH_2CH(OH)CH_2OH$)
(P)AAm	(Poly)acrylamide
MBAA	*N*,*N*′-methylenebis(acrylamide)
(P)NIPAM	(Poly)*N*-isopropylacrylamide
Irgacure 2959	2-Hydroxy-4′-(2-hydroxyethoxy)-2-methylpropiophenone
SDS	Sodium Dodecyl Sulfate
POM	Polarized Optical Microscope
DSC	Differential Scanning Calorimeter
UV	Ultraviolet Spectrophotometer
Temp	Temperature
LCST	The lower critical solution temperature

Abstract

A thermo-responsive anisotropic photonic hydrogel: poly(dodecyl glyceryl itaconate)/polyacrylamide-poly(*N*-isopropylacrylamide) hydrogel (PDGI/PAAm-PNIPAM hydrogel) has been reported. Hydrogels with uniaxially aligned lamellar bilayers possess bright structural color and swelling anisotropy, while PNIPAM-based hydrogels exhibit distinct thermo-responsive properties around a lower critical solution temperature (LCST). Hybridization of thermo-responsive PNIPAM with the lamellar hydrogel can give the anisotropic photonic hydrogel with various fascinating thermo-responsive properties, such as structural color/turbid transition, thermo-responsive structural color, and anisotropic deswelling/reswelling behavior by temperature stimuli. The temperature-induced change in turbidity, structural color, and anisotropic swelling of the gel around LCST can be tuned by controlling the incorporated PNIPAM density. PNIPAM can be regioselectively incorporated into the specific region of the lamellar hydrogels by photomasking during UV polymerization. The PDGI/PAAm-PNIPAM hydrogel can find diverse promising applications, such as smart windows and smart displays.

Chapter 1: General Introduction

Overview

Nowadays, the drastic development of thermo-responsive polymer-based smart materials has been aroused due to their unique functionalities. The most well-known and extensively researched thermo-responsive polymeric systems are aqueous poly(*N*-isopropylacrylamide) (PNIPAM) and its derivatives. Aqueous PNIPAM is classified as lower critical solution temperature (LCST)-type thermo-responsive material, which is hydrophilic below LCST but becomes hydrophobic above LCST through dehydration. This hydrophilic/hydrophobic transition at LCST imparts unprecedented properties to PNIPAM-based smart aqueous materials. For example, PNIPAM-based hydrogels exhibit transparent/turbid transition associated with the swelling/shrinking behavior upon heating and cooling process, enabling various promising applications, such as optical applications in thermo-responsive smart windows and biomedical applications in drug delivery.

On the other hand, recently hydrogels with periodically oriented two-dimensional (2-D) materials have been developed so far. Examples include hydrogels with aligned clay nanosheets, hydrogels with stacked inorganic nanosheets, and hydrogels with monodomain lamellar bilayers. Such a new class of hydrogels holds great promise as anisotropic structural materials, actuators with directional movements, and bright photonic gels owing to periodic assembly of the 2-D materials.

Outline of this thesis

Gong's group has developed an anisotropic lamellar hydrogel by entrapping thousands of self-assembled poly(dodecyl glyceryl itaconate) (PDGI) lipid bilayers inside a soft polyacrylamide (PAAm) network. The rigid and water-impermeable PDGI bilayers form a monodomain lamellar structure with a spacing of ~100 nm in the gel through the shear-flow induced self-assembly. The resulting PDGI/PAAm hydrogels with monodomain lamellar structure possess various unique properties, such as bright and tunable structure color owing to the periodic lamellar structure, high toughness owing to the rigid bilayers as sacrificial bonds, and distinct one-dimensional swelling in perpendicular to bilayer direction owing to the macroscopic orientation of the rigid bilayers.

Attempts have been made to incorporate thermo-responsive polymers into such hydrogels with 2-D materials to introduce a unique thermal response to the anisotropic hydrogels. Departing from conventional isotropic thermo-responsive hydrogels, the incorporation of thermo-responsive polymers into the anisotropic hydrogels with 2-D materials holds the potential to introduce unique functionalities and properties. For example, Miyamoto *et al.* reported the anisotropic PNIPAM hydrogel by utilizing the inorganic nanosheet liquid crystals (LCs). This anisotropic hydrogel was synthesized by radical polymerization of NIPAM in the presence of inorganic nanosheet LCs by using shear force-induced orientation. The multicomponent gels with anisotropic structure exhibit thermo-responsive anisotropic swelling and may find applications in soft actuators and sensors. Aida *et al.* developed a PNIPAM-based smart hydrogel with

oriented unilamellar titanate (IV) nanosheets (TiNS), which could undergo anisotropic deformations as a consequence of the contraction and expansion of the cofacial TiNS distance triggered by temperature. In contrast to conventional PNIPAM-based hydrogels that show homogeneous swelling/deswelling, the thermal behavior of their hydrogel, containing cofacial TiNSs, could not only be opposite (heating-induced swelling and cooling-induced shrinking) but also anisotropic. These innovations, stemming from the synergy of thermo-responsiveness and anisotropic structures, could open up a new chapter in material science.

As mentioned above, this research goal is to introduce thermo-responsive PNIPAM polymers into photonic PDGI/PAAm lamellar gels, so we can facilely not only tune the turbidity driven by phase separation behavior but also control the properties of PDGI/PAAm gels, such as tunable structural color and anisotropic swelling by temperature stimuli around LCST. Furthermore, to investigate the effect of incorporated PNIPAM concentration on the properties of the hydrogel, including anisotropic swelling, structural color tunability, and reversibility.

In **Chapter 2**, the research background of this research topic (Reversible tuning of turbidity, structural color, and anisotropic swelling in thermo-responsive lamellar hydrogel) is summarized.

In **Chapter 3**, the strategy towards introducing thermo-responsive PNIPAM polymers into photonic PDGI/PAAm lamellar gels is introduced in detail and the synthetic procedure of PDIG/PAAm-PNIPAM hydrogel is included. The thermo-induced phase separation behavior of PDGI/PAAm-PNIPAM gel is introduced.

Importantly, the PDGI/PAAm-PNIPAM hydrogel shows tunable structural color ability by controlling incorporated PNIPAM concentration.

In **Chapter 4**, the anisotropic lamellar structure and deswelling/reswelling behaviors of PDGI/PAAm-PNIPAM gels during heating and cooling process around LCST was discussed. The PDGI/PAAm-PNIPAM hydrogel with different NIPAM concentration was synthesized.

In **Chapter 5**, the effect of PNIPAM concentration on PDGI/PAAm-PNIPAM gel during heating and cooling process around LCST is introduced in detail, including on the ultrafast turbidity, structural color, interplanar distance, anisotropic swelling, and reversibility.

In **Chapter 6**, the synthesis procedure of pattern PDGI/PAAm-PNIPAM in PDGI/PAAm hydrogel is described in detail. The structure color/turbid transition of the gel pattern during heating and cooling process around LCST is investigated. The applications of the pattern gel are also introduced.

In **Chapter 7**, conclusions of the whole dissertation are summarized.

Chapter 2: Background

2.1 Thermo-responsive PNIPAM-based smart hydrogel

PNIPAM is one of the most fascinating and popular thermo-responsive polymers that have attracted extensive research interest.[1-3] PNIPAM is extended in cold water due to its inter- and intramolecular hydrogen bonding but phase separates upon heating at *Temp* > 33 ℃, which is its lower critical solution temperature (LCST). When the temperature is lower than the LCST of PNIPAM, the hydrogen bonds between the hydrophilic amide groups and water molecules counteract the hydrophobic interactions between the isopropyl groups that cause the collapse of PNIPAM chain to avoid contact with water (**Figure 2-1**).[2] In this case, PNIPAM becomes hydrophilic and dissolved in aqueous solution wherein polymer chains display flexible and expanded random-coil conformations. With increasing temperature even to higher than the LCST, the hydrogen bonds are weakened and the hydrophilic interactions among the isopropyl groups becomes strong, leading to a more unfavorable entropy contribution to the free energy. In this case, an entropy-driven phase separation occurs, wherein PNIPAM chains are dehydrated and aggregate into a tightly packed globular conformation. From the perspective of thermodynamic principles, the LCST of PNIPAM can be manipulated across a wide temperature range through incorporation of a more hydrophilic component or a hydrophobic monomer via copolymerization to effectively change the enthalpic contribution to the thermal response.[3]

PNIPAM-based smart hydrogels exhibit distinct thermo-responsive properties near LCST, which have found diverse promising applications such as smart coating, drug delivery, tissue regeneration, and artificial muscles.[1] For example, PNIPAM-based smart hydrogels are a promising class of materials that demonstrate unique properties, such as temperature-induced changes in volume near their LCST and exhibit hydrophilicity and transparency resulting from the phase separation transition around LCST.[4-6] It is worth mentioning that the property changes of PNIPAM-based smart hydrogels can be triggered through various stimuli, including direct/indirect heating[7-9], photoionization[10], or photoisomerization[11], making them sensitive to changes in temperature, light, electrical field, and magnetic field. The ability of PNIPAM-based smart hydrogels to undergo reversible changes in response to external stimuli makes them highly suitable for applications in drug delivery, tissue engineering, sensors, and other fields where precise control over material properties is required.[5,12-21] The extensive research on PNIPAM-based smart hydrogels and their diverse stimulus responsiveness make them a promising area of study with significant potential for further advancements and practical applications, such as smart actuators in gripper, soft walker and bionic motion; optical applications in smart window, smart display, and anticounterfeiting; biomedical applications in drug delivery, cell scaffold and cell sheeting, etc (**Figure 2-2**).[12-21]

PNIPAM-based hydrogels, however, have inherent drawbacks such as isotropic structure, limited drug loading capacity, and low mechanical strength.[22] The most effective strategies to improve the properties of PNIPAM-based hydrogels is to

incorporate functional inorganic nanoparticles or self-assembled structures to give composite hydrogels and linking PNIPAM networks with other polymer chains of unique properties to process copolymeric hydrogels.[23,24] After incorporating or copolymerization, the resulting hydrogel could have combined properties and abilities.

2.2 Smart photonic hydrogels

Recently, photonic hydrogels have gained significant attention in the field of sensors owing to their unique optical properties that stem from their periodically ordered structure. Photonic hydrogels, which possess a three-dimensional polymer network structure have additional advantages as active chromatic materials through swelling/deswelling in response to environmental stimuli, such as pH, solvent, and temperature (**Figure 2-3 & Figure 2-4**).[25-33] Responsive photonic crystals are dielectrically periodical structures that can alter their diffraction wavelength upon exposure to chemical or physical stimuli, such as pH, ionic strength, solvent, and electric and magnetic fields.[34-36] The photonic hydrogels are promising materials used as intelligent sensors to show a color change in response to one or even multiple environmental stimuli.[36]

Recently, our group has developed an anisotropic photonic hydrogel (PDGI/PAAm) with lamellar structure by entrapping self-assembled single-domain lamellar bilayers inside a soft polyacrylamide (PAAm) layer (**Figure 2-5** and **Figure 2-6**).[34-40] The rigid, water-impermeable bilayers, poly(dodecyl glyceryl itaconate) (PDGI), self-assembled into a periodic structure inside the PAAm layers by applying shear flow to diffract light

and also serve as reversible sacrificial bonds to toughen the gel. The resulting PDGI/PAAm hydrogel with lamellar structure, not only possesses excellent structure color and color tunability by polymerization with another component to the gels, but also exhibits distinct one-dimensional swelling along the thickness direction owing to the presence of macroscopic bilayers. Although, anisotropic photonic hydrogels are promising materials for displays and sensors, hydrogels generally have poor functionality, primarily due to differences in their microstructures.

2.3 Inspiration and strategy

Nowadays, various attempts have been made to incorporate PNIPAM networks into internal anisotropic hydrogels.[22,41,42] After being integrated into internal anisotropic hydrogels or been fabricated into periodic structures, the size change of PNIPAM-based smart hydrogels can realize shape change functions or enable the tunable vivid coloration reproducing the iridescence or structural colors in the nature, which find numerous applications for the development of smart optical sensors, smart coating, drug delivery, tissue regenerating, and artificial muscles (**Figure 2-7**).[1,24] Nevertheless, introducing thermo-responsive PNIPAM polymers into anisotropic photonic hydrogels with lamellar structure to achieve not only phase separation behavior but also anisotropic swelling and structural color tunability is seldom realized.

In this work, this research goal is to incorporate PNIPAM as the thermo-responsive component into PDGI/PAAm lamellar hydrogels to form PDGI/PAAm-PNIPAM hydrogels with unique thermo-responsive optical and swelling properties. In this

resulting gel, we can facilely not only tune the turbidity driven by phase separation behavior but also control the properties of PDGI/PAAm gels, such as tunable structural color and anisotropic swelling by temperature stimuli around LCST. Furthermore, the effect of incorporated PNIPAM concentration on the properties of the hydrogel has also been investigated, including anisotropic swelling, structural color tunability, and reversibility.

Reference

[1] L. Tang, L. Wang, X. Yang, Y. Feng, Y. Li, W. Feng. Poly(N-isopropylacrylamide)-based Smart Hydrogels: Design, Properties and Applications. *Prog. Mater. Sci.* **2021**, 115, 110702.

[2] F. Doberenz, K. Zeng, C. Willems, K. Zhang, T. Groth. Thermoresponsive Polymers and their Biomedical Application in Tissue Engineering - A Review *J. Mater. Chem. B* **2020**, 8, 607-628.

[3] Y. Ding, X. Zhang, B. Xua, W. Li. LCST and UCST-type Thermoresponsive Behavior in Dendronized Gelatins. *Polym. Chem.* **2022**, 13, 2813-2821.

[4] L.W. Xia, R. Xie, X.J. Ju, W. Wang, Q. Chen, L.Y. Chu. Nano-Structured Smart Hydrogels with Rapid Response and High Elasticity. *Nat. Commun.* **2013**, 4, 2226.

[5] O. Erol, A. Pantula, W. Liu, D.H. Gracias. Transformer Hydrogels: A Review. *Adv. Mater. Technol.* **2019**, 4, 1900043.

[6] Y. S. Kim, M. Liu, Y. Ishida, Y. Ebina, M. Osada, T. Sasaki, T. Hikima, M. Takata, T. Aida. Thermoresponsive Actuation Enabled by Permittivity Switching in an Electrostatically Anisotropic Hydrogel. *Nat. Mater.* **2015**, 14, 1002-1007.

[7] Y. Zhao, C. Xuan, X. Qian, Y. Alsaid, M. Hua, L. Jin, X. He. Soft Phototactic Swimmer Based on Self-Sustained Hydrogel Oscillator. *Sci. Robot* **2019**, 4, eaax7112.

[8] Z. Zhao, H. Wang, L. Shang, Y. Yu, F. Fu, Y. Zhao, Z. Gu. Bioinspired Heterogeneous Structural Color Stripes from Capillaries. *Adv. Mater.* **2017**, 29, 1704569.

[9] C. Yu, Z. Duan, P. Yuan, Y. Li, Y. Su, X. Zhang, Y. Pan, L. L. Dai. Electronically Programmable, Reversible Shape Change in Two- And Three-Dimensional Hydrogel Structures. *Adv. Mater.* **2013**, 25, 1541-1546.

[10] A. Mamada, T. Tanaka, D. Kungwatchakun, M. Irie. Photoinduced Phase Transition of Gels. *Macromolecules* **1990**, 23, 1517-1519.

[11] T. Satoh, K. Sumaru, T. Takagi, T. Kanamori. Fast-Reversible Light-Driven Hydrogels Consisting of Spirobenzopyran-Functionalized Poly(N-Isopropylacrylamide). *Soft Matter* **2011**, 7, 8030-8034.

[12] T. Sun, W. Song, L. Jiang. Control Over the Responsive Wettability of Poly(N-Isopropylacrylamide) Film in A Large Extent by Introducing an Irresponsive Molecule. *Chem. Commun.* **2005**, 13, 1723-1725.

[13] M. Wang, Y. Gao, C. Cao, K. Chen, Y. Wen, D. Fang, L. Li, X. Guo. Binary Solvent Colloids of Thermosensitive Poly(N-Isopropylacrylamide) Microgel for Smart Windows. *Ind. Eng. Chem. Res.* **2014**, 53, 18462-18472.

[14] G. Gao, Z. Wang, D. Xu, L. Wang, T. Xu, H. Zhang, J. Chen, J. Fu. Snap-Buckling Motivated Controllable Jumping of Thermo-Responsive Hydrogel Bilayers. *ACS Appl. Mater. Interfaces.* **2018**, 10, 41724-41731.

[15] X-H. Li, C. Liu, S-P. Feng, N. X. Fang Broadband Light Management with Thermochromic Hydrogel Microparticles for Smart Windows. *Joule* **2019**, 3, 290-302.

[16] W. J. Zheng, N. An, J. H. Yang, J. Zhou, Y. M. Chen. Tough Al-alginate/Poly(N-isopropylacrylamide) Hydrogel with Tunable LCST for Soft Robotics. *ACS Appl. Mater. Interfaces* **2015**, 7, 1758-1764.

[17] H. Arslan, A. Nojoomi, J. Jeon, K. Yum. 3D Printing of Anisotropic Hydrogels with Bioinspired Motion. *Adv. Sci.* **2019**, 6, 1800703.

[18] M. C. Chiappelli, R. C. Hayward. Photonic Multilayer Sensors from Photo-Crosslinkable Polymer Films. *Adv. Mater.* **2012**, 24, 6100-6104.

[19] X. Cheng, Y. Jin, T. Sun, R. Qi, B. Fan, H. Li. Oxidation- and Thermo-Responsive Poly(N-isopropylacrylamide-co-2-Hydroxyethyl Acrylate) Hydrogels Cross-Linked via Diselenides for Controlled Drug Delivery. *RSC Adv.* **2015**, 5, 4162-4170.

[20] Y-J. Kim, M. Ebara, T. Aoyagi. A Smart Nanofiber Web That Captures and Releases Cells. *Angew. Chem. Int. Ed.* **2012**, 51, 10537-10541.

[21] Y. Tsuda, A. Kikuchi, M. Yamato, G. Chen, T. Okano. Heterotypic Cell Interactions on A Dually Patterned Surface. *Biochem. Biophys. Res. Commun.* **2006**, 348, 937-944.

[22] M. A. Haq, Y. Su, D. Wang. Mechanical Properties of PNIPAM Based Hydrogels: A Review. *Mater. Sci. Eng. C* **2017**, 70, 842-855.

[23] Q. Zhao, X. Yang, C. Ma, D. Chen, H. Bai, T. Li, W. Yang, T. Xie. A Bioinspired Reversible Snapping Hydrogel Assembly. *Mater. Horiz.* **2016**, 3, 422-428.

[24] G. Isapour, M. Lattuada. Bioinspired Stimuli-Responsive Color-Changing Systems. *Adv. Mater.* **2018**, 30, 1707069.

[25] Y. Kang, J. J Walish, T. Gorishnyy, E. L Thomas. Broad-Wavelength-Range Chemically Tunable Block-Copolymer Photonic Gels. *Nat Mater.* **2007**, 6, 957-960.

[26] A. C. Arsenault, D. P. Puzzo, I. Manners, G. A. Ozin. Photonic-Crystal Full-Colour Displays. *Nat. Photon.* 2007, 1, 468-472.

[27] Y. J. Lee, P. V. Braun. Tunable Inverse Opal Hydrogel pH Sensors. *Adv. Mater.* **2003**, 15, 563-566.

[28] A. C. Arsenault, T. J. Clark, G. von Freymann, L. Cademartiri,R. Sapienza, J. Bertolotti, E. Vekris, S. Wong, V. Kitaev, I. Manners,R. Z. Wang, S. John, D. Wiersma, G. A. Ozin. From Colour Fingerprinting to the Control of Photoluminescence in Elastic Photonic Crystals. *Nat. Mater.* **2006**, 5 ,179-184.

[29] J. T. Zhang, L. L. Wang, J. Luo, A. Tikhonov, N. Kornienko, S. A. Asher. 2-D Array Photonic Crystal Sensing Motif. J. *Am. Chem. Soc*. **2011**, 133, 9152-9155.

[30] Y. Ahn, E. Kim, J. Hyon, C. Kang, Y. Kang. Photoresponsive Block Copolymer Photonic Gels with Widely Tunable Photosensitivity by Counter-Ions. *Adv. Mater.* **2012**, 24, OP127-OP130.

[31] I. B. Burgess, L. Mishchenko, B. D. Hatton, M. Kolle, M. Loncar, J. Aizenberg. Encoding Complex Wettability Patterns in Chemically Functionalized 3D Photonic Crystals. *J. Am. Chem. Soc.* **2011**, 133, 12430-12432.

[32] H. Kim, J. P. Ge, J. Kim, S. Choi, H. Lee, W. Park, Y. Yin, S. Kwon. Structural Colour Printing Using a Magnetically Tunable and Lithographically Fixable Photonic Crystal. *Nat. Photon.* **2009,** 3, 534-540.

[33] K. Matsubara, M. Watanabe, Y. Takeoka. A Thermally Adjustable Multicolor Photochromic Hydrogel. *Angew. Chem. Int. Ed.* **2007**, 46, 1688-1692.

[34] M. A. Haque, G. Kamita, T. Kurokawa, K. Tsujii, J. P. Gong. Unidirectional Alignment of Lamellar Bilayer in Hydrogel: One-Dimensional Swelling, Anisotropic Modulus, and Stress/Strain Tunable Structural Color. *Adv. Mater.* **2010**, 22, 5110-5114.

[35] M. A. Haque, T. Kurokawa, G. Kamita, Y. Yue, J. P. Gong. Rapid and Reversible Tuning of Structural Color of a Hydrogel over the Entire Visible Spectrum by Mechanical Stimulation. *Chem. Mater.* **2011**, 23, 5200-5207.

[36] Y. F. Yue, M. A. Haque, T. Kurokawa, T. Nakajima, J. P. Gong. Lamellar Hydrogels with High Toughness and Ternary Tunable Photonic Stop-Band. *Adv. Mater.* **2013**, 25, 3106-3110.

[37] M. A. Haque, K. Mito, T. Kurokawa, T. Nakajima, T. Nonoyama, M. Ilyas, J. P. Gong. Tough and Variable-Band-Gap Photonic Hydrogel Displaying Programmable Angle-Dependent Colors. *ACS Omega* **2018**, 3, 55-62.

[38] X. Li, T. Kurokawa, R. Takahashi, M. A. Haque, Y. Yue, T. Nakajima, J. P. Gong. Polymer Adsorbed Bilayer Membranes Form Self-Healing Hydrogels with Tunable Superstructure. *Macromolecules* **2015**, 48, 2277-2282.

[39] Y. Yue, T. Kurokawa, M. A. Haque, T. Nakajima, T. Nonoyama, X. Li, I. Kajiwara, J. P. Gong. Mechano-Actuated Ultrafast Full-Colour Switching in Layered Photonic Hydrogels. *Nat. Commun.* **2014**, 5, 4659.

[40] M. A. Haque, T. Kurokawa, J. P. Gong. Anisotropic Hydrogel Based on Bilayers: Color, Strength, Toughness, and Fatigue Resistance. *Soft Matter* **2012**, 8, 8008-8016.

[41] X. Le, W. Lu, J. Zhang, T. Chen. Recent Progress in Biomimetic Anisotropic Hydrogel Actuators. *Adv.Sci.* **2019**, 6, 1801584.

[42] A. S. Gladman, E. A. Matsumoto, R. G. Nuzzo, L. Mahadevan, J. A. Lewis. Biomimetic 4D Printing. *Nat. Mater.* 2016, 15, 413-417.

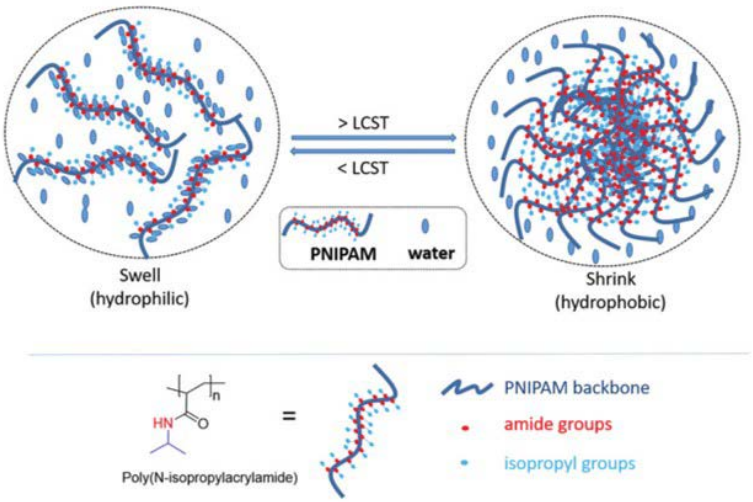

Figure 2-1: Graphical representation of thermoresponsive LCST behaviour of PNIPAM.

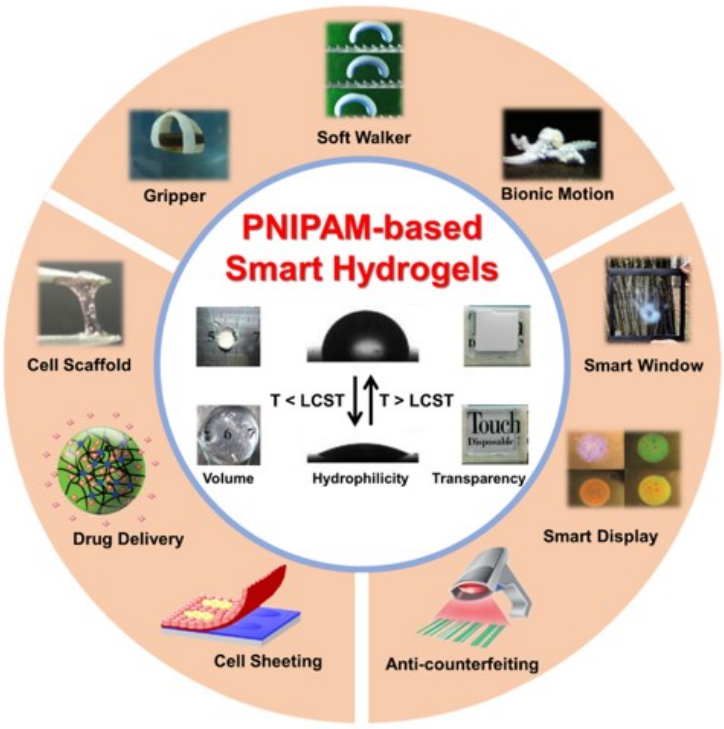

Figure 2-2: Representative thermo-responsive properties (e.g., temperature-induced changes in volume, hydrophilicity and transparency around the LCST) and applications (e.g., smart actuators in gripper, soft walker and bionic motion; optical applications in smart window, smart display, and anticounterfeiting; biomedical applications in drug delivery, cell scaffold and cell sheeting, etc.) of PNIPAM-based smart hydrogels.

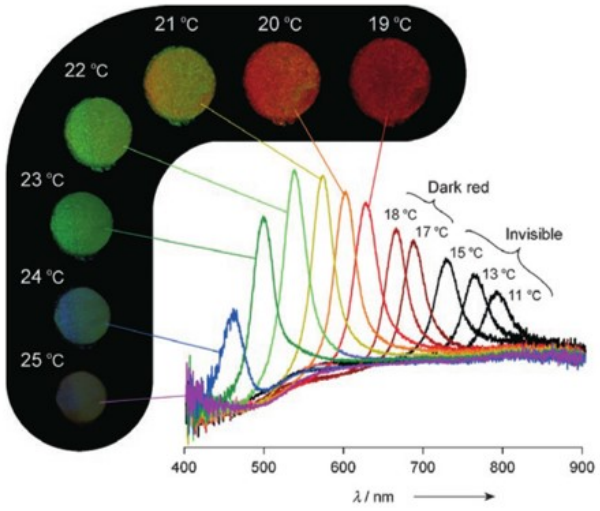

Figure 2-3: Spectroscopic characterization of the porous gel. Photographs and reflection spectra of the porous poly(NIPA-co-AAB) gel in the dark at various temperatures.

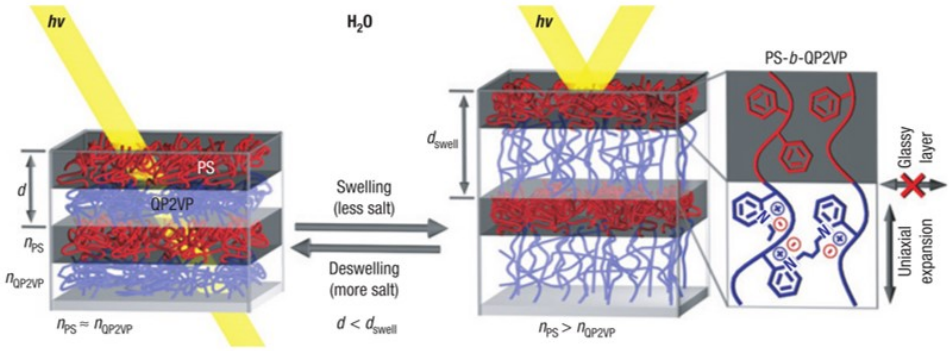

Figure 2-4: Schematic diagram of the structure of photonic gel film and the tuning mechanism. The photonic gel film was prepared by self-assembly of a deblock copolymer (PS-b-QP2VP). Swelling/deswelling of the QP2VP gel layers (blue) by aqueous solvents modulates both the domain spacing and the refractive-index contrast, and accordingly shifts the wavelengths of light (hv) reflected by the stop band. The hydrophobic and glassy polystyrene layers (red) limit expansion of the gel layers to the direction normal to the layers.

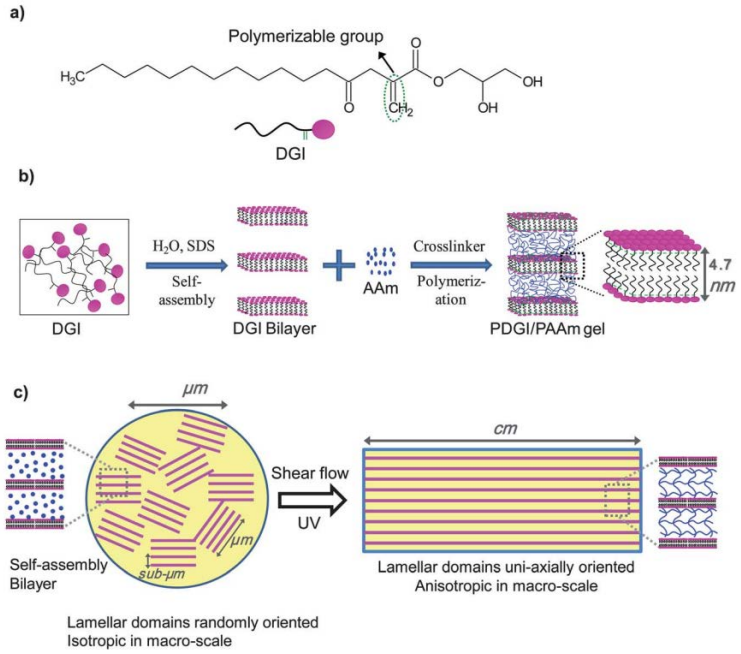

Figure 2-5: (a) Molecular structure of dodecyl glyceryl itaconate (DGI) containing a polymerizable double bond. (b) In the presence of an ionic surfactant, sodium dodecyl sulfate (SDS), DGI molecules self-assemble into a lamellar bilayer structure in water. This structure is retained in an aqueous solution of acrylamide (AAm) in the presence of a cross-linker and an initiator. By polymerization, polymeric-DGI (PDGI) lamellar bilayers are entrapped inside the amorphous polyacrylamide (PAAm) network and the hybrid PDGI/PAAm hydrogel is obtained. (c) Prior to the polymerization, randomly oriented self-assembled lamellar bilayer domains are aligned in one direction (anisotropic in the macro-scale) by shear flow to the precursor solution.

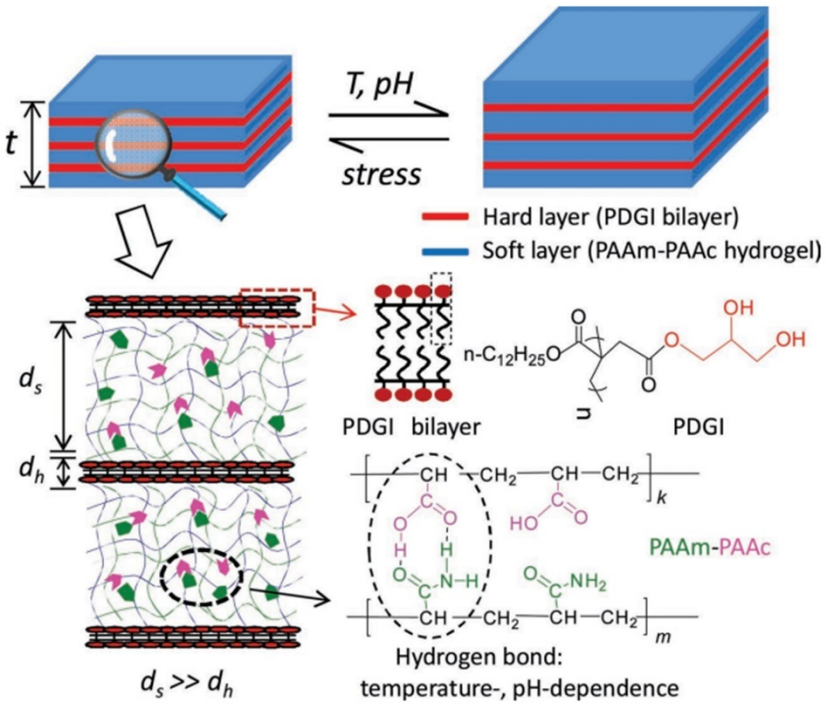

Figure 2-6. Illustration of the ternary stimuli-responsive photonic hydrogel, PDGI/PAAm–PAAc, based on an alternating soft and hard layer structure. The hard and non-water permeable layer consists of a polymeric surfactant PDGI bilayer with a thickness (d_h) of 4.7 nm. The soft and swellable layer is an interpenetrating network of PAAm–PAAc with a thickness (d_s) of several hundreds of nanometers, which varies with external stimuli such as temperature, pH, and mechanical stress/strain. The soft layers swell with increases in temperature and pH, due to dissociation of the hydrogen bonds between the two networks and the ionization of PAAc, which leads to a red-shift of the photonic stop-bands. From the thickness (t) of the gel and the reflection peak, λ_{max}, the number of lamellar layers in the gel is estimated as ≈ 4000 using Bragg's relation.

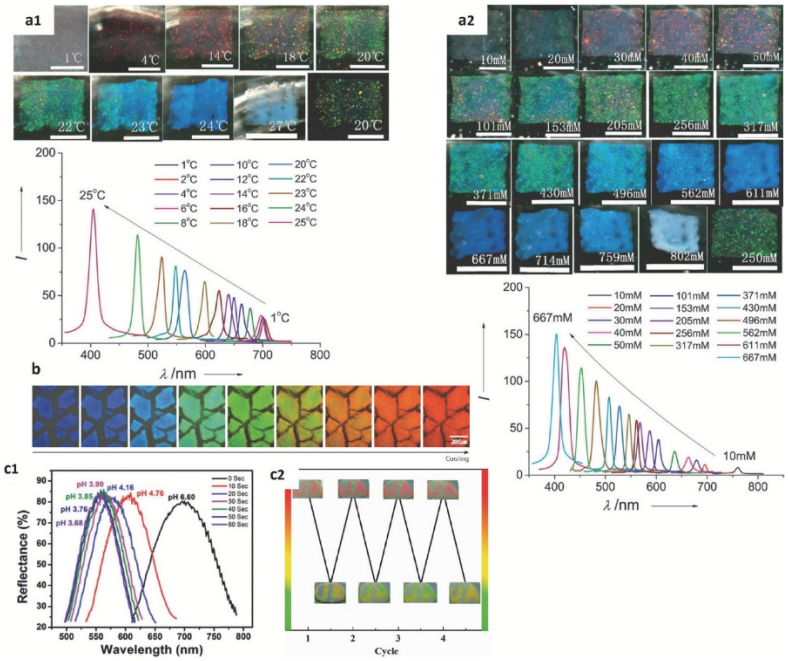

Figure 2-7: Color change patterns of P(NIPAM-AAc) systems. a) Photographs and reflection spectra of free-standing colloidal crystals films of HEMA-modified P(NIPAM-AAc) microgels: a_1) temperature increase. At the bottom right, the film was cooled back to 20 °C. The film was immersed in 0.5 m NaCl solution, pH 3.0. Scale bar is 0.5 cm. a_2) [NaCl] increase. At the bottom right [NaCl] was decreased back to 250 × 10^{-3} M. Scale bar is 0.5 cm, pH 3.0. *Temp* = 23 °C. b) A uniform change of structural color in optical microscopy images of PS/P(NIPAM-AAc) hydrogel photonic crystals upon heating from 20 to 40 °C. c) Reflectance spectrum for a P(NIPAM-AAc)-based etalon in *o*-nitrobenzaldehyde (*o*-NBA) solution: c_1) after exposure to UV irradiation for the indicated times, color reversibility by repeated exposure to UV irradiation, c_2) followed by the addition of fresh *o*-NBA solution.

Chapter 3: Synthesis of thermo-responsive lamellar hydrogel

3.1 Introduction

In this work, the synthesis of PDGI/PAAm hydrogels were synthesized according to our previous work.[1] The molecular formula in this work was shown in **Figure 3-1**. Herein the PDGI/PAAm-PNIPAM gels were synthesized by incorporating second networks (PNIPAM) into PAAm soft layers of PDGI/PAAm lamellar gels. The schematic illustration of fabrication and property of PDGI/PAAm-PNIPAM hydrogel were shown in **Figure 3-2**. The chemical structure of PDGI bilayer, PAAm layer and PAAm-PNIPAM layer were shown in **Figure 3-2 (left side)**. The PDGI/PAAm-PNIPAM gel exhibits thermo-induced phase separation behavior. By incorporating PNIPAM network into PAAm layer to give PDGI/PAAm-PNIPAM lamellar hydrogel fast reversible phase separation ability (**Figure 3-3** and **Figure 3-4**). This hybrid hydrogel has a hard PDGI bilayer and soft PAAm-PNIPAM layer. At *Temp* > LCST, PNIPAM networks becomes hydrophobic and gels show turbid phenomenon immediately, but the interplanar distance of the gel decreases gradually with releasing water owing to the presence of macroscopic bilayers (**Figure 3-5**); at *Temp* < LCST, PNIPAM becomes hydrophilic and turbidity disappears immediately, but the interplanar distance increases gradually absorbing water to reach the original/swollen state, discussed in **Chapter 4-6**. The PDGI/PAAm-PNIPAM hydrogel shows tunable structural color ability by controlling incorporated PNIPAM concentration. The

successful incorporation can be confirmed by DSC thermograms of PDGI/PAAm and PDGI/PAAm-PNIPAM gels with different PNIPAM concentration (**Figure 3-6**). The gel shows a red shift in color after incorporation and with increasing the PNIPAM concentration, the gel shows a larger red shift in color and gel thickness (**Figure 3-7 and Figure 3-8**). The effect of the incorporated PNIPAM concentrations on the thermo-responsive lamellar hydrogel during the heating and cooling processes is discussed in **Chapter 4-5**.

3.2 Experiments

3.2.1 Materials

An amphiphilic monomer, dodecyl glyceryl itaconate [DGI (*n*-$C_{12}H_{25}$-$OCOCH_2C$-(=CH_2)$COOCH_2CH(OH)CH_2OH$)], was synthesized following the procedure described earlier.[1] After completion of two-step reactions, the crude product was purified at least twice by a silica gel column (silica gel 60 N, Kanto Chemical Co., Inc.). The DGI fraction was eluted with a hexane/ethyl acetate mixture (1:1 by volume) and was further purified twice by recrystallization from an acetone/hexane mixture (1/1 by weight). *N*,*N*′-methylenebis(acrylamide) (MBAA, 99.0%, FUJIFILM Wako Pure Chemical Corporation, Japan) was recrystallized from ethanol, acrylamide (AAm, 98%, JUNSEI Chemicals Co. Ltd., Japan) was recrystallized from chloroform, *N*-isopropylacrylamide (NIPAM, 97%, Sigma-Aldrich Co., USA) was recrystallized twice from an ether/hexane mixture. 2-Hydroxy-4′-(2-hydroxyethoxy)-2-methylpropiophenone (Irgacure 2959, 98%, Sigma-Aldrich Co., USA) and sodium

dodecyl sulfate (SDS, 98%, FUJIFILM Wako Pure Chemical Corporation, Japan) were used as received. Milli-Q deionized water was used to prepare the monomer solutions and for the swelling of the gel. The molecular formula of the monomer, corss-linker and initiater was presented in **Figure 3-1**.

3.2.2 Preparation of PDGI/PAAm gel

PDGI/PAAm hydrogels were prepared by simultaneous free-radical polymerization from an aqueous solution of 0.10 M DGI, 0.025 mM SDS, 4 M AAm, 4 mM MBAA as a cross-linker of AAm, and 2 mM Irgacure 2959 as a photoinitiator. The detailed procedure was described in our previous papers.[1-3] In short, a glass bottle with mixture of the precursors and water was allowed to stand in a 55 ℃ (above the Krafft point of DGI at 43 ℃) water bath for 10 min and apply gentle shear to the mixture to dissolve DGI powders. Then the solution was kept again in a 55 ℃ water bath for 5 h to form stable lamellar bilayers of the self-assembled DGI with trace SDS. Then the solution was transferred to a glove box filled with argon to remove dissolved oxygen in the solution. A sheet-like PDGI/PAAm hydrogel ($15 \times 7 \times 0.5$ cm^3) with a monodomain multilamellar structure parallel to the sheet surface was achieved following the same procedure described in our previous paper.[3] Briefly, prior to the polymerization, the precursor solution was poured to the glass substrate with a shear flow to align thousands of lamellar bilayers of self-assembled DGI parallel to the surface of the glass substrate. After UV polymerization of DGI and AAm, bilayers of polymerized PDGI were entrapped in the PAAm matrix to give an anisotropic and

mechanically tough hydrogel. After attaining swelling equilibrium in water, a greenish PDGI/PAAm gel was obtained.

3.2.3 Preparation of PDGI/PAAm-PNIPAM gel

In the second step, the green PDGI/PAAm gel was immersed in an aqueous solution of *c* M NIPAM, 0.05 mM MBAA and 0.05 mM Irgacure 2959 for 7 days to reach equilibrium. *c* is called feed concentration of NIPAM of the precursor solution. *c* was set to 0, 0.25, 0.5, and 1.0 M considering the highest solubility of NIPAM in water at room temperature. During solvent exchange from water to the NIPAM solution, a large shrinkage of the thickness of the gel as well as a blue-shift of the structural color were observed probably because NIPAM aqueous solution is a relatively poor solvent for the gel, causing the gel to lose water. By performing a second UV polymerization of NIPAM in the presence of the PDGI/PAAm gel at 4 °C for 8 h, the PNIPAM network was formed within the PAAm network and an interpenetrating network structure was constructed. The obtained gels are coded as PDGI/PAAm-PNIPAM$_{c\mathrm{M}}$ hydrogel. The thus-obtained PDGI/PAAm-PNIPAM$_{0.5\mathrm{M}}$ gel exhibited a blue color in the as-prepared state. After attaining equilibrium swelling in water for 7 days, the gel shows a red shift in color (red color) at room temperature. The water content of the gel is ≈ 93 wt%. The illustration of the reversibly thermal-responsive anisotropic photonic hydrogel based on lamellar structure, PDGI/PAAm-PNIPAM$_{0.5\mathrm{M}}$ is shown in **Figure 3-2**. The turbidity of PDGI/PAAm-PNIPAM gel during heating and cooling process around LCST is

controllable by controlling incorporated PNIPAM concentrations, as revealed by the **Figure 3-3**.

3.2.4 Transmittance Analysis

The transmittance of the sample was measured using an ultraviolet/visible light spectrophotometer (UV-1800, SHIMADZU, Japan) with a temperature control device. The sheet-like gel sample was placed in a quartz cuvette filled with water during measurement. The light was imposed to the top surface of the lamellar gels. The range of 400-700 nm is the wavelength range of visible light. The transmittance spectra of the samples in the range of 400-700 nm was measured.

To compare the transmittance in the range of 400-700 nm above and below LCST of PDGI/PAAm-PNIPAM hydrogel samples, a temperature control device was installed and the transmittance from 20 to 70 °C was measured (**Figure 3-4**). To compare the turbidity of the gel after incorporated PNIPAM networks, the transmittance of PDGI/PAAm-PNIPAM$_{0.5M}$ was measured in the range of 400-700 nm during heating process at 50 °C (**Figure 3-5**). The UV light was imposed to the top surface of the lamellar gels. The sample was placed in a quartz cuvette filled with water during measurement.

3.2.5 Thermal Analysis

The lower critical solution temperature (LCST) of PDGI/PAAm-PNIPAM hydrogels were measured using a differential scanning calorimeter (DSC 2500, TA instrument, USA) under a nitrogen atmosphere. The heat rate was 3 ºC min^{-1}. The

temperature at which phase transition occurs, LCST, was measured as peak temperature of an exothermic reaction.

To verify the incorporation of PNIPAM networks into PAAm soft layers, the DSC of PDGI/PAAm, PDGI/PAAm-PNIPAM$_{0.25M}$, PDGI/PAAm-PNIPAM$_{0.5M}$, and PDGI/PAAm-PNIPAM$_{1.0M}$ were measured and shown in **Figure 3-6**.

3.2.6 Thickness Measurement

The thickness of the PDGI/PAAm and PDGI/PAAm-PNIPAM gels, *T*, was measured using a mechanical thickness meter (Teclck, Dumb Bell Ltd., Japan).

3.2.7 Reflection spectrum

Reflection spectra of various gel samples were measured by a combined setup of a light source, variable angle measurement device, and an analyzer. An Xe lamp was used as a light source to obtain the reflection spectrum. Reflection measurement optics with variable angles (Hamamatsu Photonics KK, C10027A10687) were used to detect the reflected light. A photonic multichannel analyzer (Hamamatsu Photonics KK, C10027) was used for analyzing the detected signals. The entire reflection spectrum was obtained by keeping the incident angle at 60° and reflection angles at 45°. The distance between two lamellar layers, *d*, was roughly calculated using Bragg's law of diffraction, $\lambda_{max} = 2nd\sin\theta$, where $n = 1.33$ is the refractive index of water, θ is the incident angle, and λ_{max} is the wavelength at maximum reflectance intensity.[3] Reflection spectra of PDGI/PAAm and PDGI/PAAm-PNIPAM hydrogels synthesized

with different NIPAM feed concentration in pure water at room temperature was shown in **Figure 3-8**.

3.3 Results and discussion

3.3.1 Strategy for synthesis of thermo-responsive lamellar hydrogel

The schematic illustration of fabrication and property of PDGI/PAAm-PNIPAM hydrogels were shown in **Figure 3-2**. In this work, we incorporate PNIPAM as the thermo-responsive component into PDGI/PAAm lamellar hydrogels to form PDGI/PAAm-PNIPAM hydrogels with unique thermo-responsive optical and swelling properties. PNIPAM is incorporated into the PAAm layer of PDGI/PAAm hydrogels to form an interpenetrating soft layer of PAAm-PNIPAM (**Figure 3-2**) inside the hydrogels while maintaining the anisotropic structure. As introduced above, aqueous PNIPAM undergoes a temperature-driven, reversible LCST-type phase transition. Below the LCST, it is water-soluble owing to strong hydrogen bonds between the amide groups and the water molecules. Above the LCST, weakened hydrogen bonds and strengthened hydrophobic interactions instantly make the PNIPAM chains contract into hydrophobic globules, making the system turbid.[4-8] Introduction of a thermo-responsive PNIPAM network into the hydrophilic PAAm to form an interpenetrating network negligibly affects the phase separation and LCST of PNIPAM, suggesting a negligible effect of the PNIPAM-PAAm interaction on the phase separation.[9] As a consequence, after the introduction of the PNIPAM network into the lamellar hydrogels, turbidity of such photonic PDGI/PAAm-PNIPAM hydrogels can be instantly tuned

with temperature. The incoporation of PNIPAM networks into the soft PAAm layers, increases the interplanar distance of the hydrogel, therefore the gel shows a red shift in color from green to red. The introduced PNIPAM is hydrolyzed in cold water but turns water-insoluble upon heating.[10-15] As a consequence, we can facilely tune the turbidity of the photonic PDGI/PAAm-PNIPAM hydrogels with temperature, leading the structure color/turbid transition of the gel at LCST. Moreover, since dehydrolyzation of PNIPAM in the gel at high temperature also leads deswelling of the whole gel, swelling ratio of the PDGI/PAAm-PNIPAM hydrogels can also be tuned by temperature, leading tunable structural color and anisotropic swelling by temperature stimuli around LCST. The effect of incorporated PNIPAM density on the properties of the hydrogel has also been investigated, including turbidity, swelling anisotropy, structural color tunability, and reversibility of them (**Chapter 4-5**).

3.3.2 Thermo-induced phase separation behavior

PNIPAM as a temperature-responsive polymer, is extended in cold water due to its inter- and intramolecular hydrogen bonding but phase separates upon heating at *Temp* > 33 ℃, which is its LCST.[10,11] The photographs of PDGI/PAAm-PNIPAM$_{0.5M}$ gel in pure water at different temperatures is shown in **Figure 3-3**. At room temperature and *Temp* = 30 ℃, the PDGI/PAAm-PNIPAM$_{0.5M}$ gel shows no turbidity and exhibits structural color. At *Temp* = 40 and 50 ℃, the gel turns turbid immediately once immersed in hot water. The hydrogel exhibits lower turbidity in 40 ℃ hot water

compared to 50 °C hot water. It indicates that the turbidity PDGI/PAAm-PNIPAM hydrogel is determined by the heating temperature.

The effect of heating temperature on the transmittance of the PDGI/PAAm-PNIPAM$_{0.5M}$ gel was shown in **Figure 3-4**. The original gel (*Temp* = 20 ℃) exhibited high transmittance at 400 nm. By increasing heating temperature from 20 to 80 ℃, the transmittance of the gel dropped dramatically when heating temperature reaches to ~33 ℃ and then reached a plateau. This corresponds to the LCST-type thermo-responsive behavior of the gels. The hydrogels undergo phase separation when heating temperature is above the LCST due to entropy-driven dehydration and collapse upon heating (**Figure 3-3**).[10,11]

The effect of heating time on the transmittance of PDGI/PAAm-PNIPAM$_{0.5M}$ gel is shown in **Figure 3-5**. The transmittance of the PDGI/PAAm-PNIPAM$_{0.5M}$ gel during heating process at 50 ℃ in the range of 400-700 nm was measured to quantify the characteristics of the turbidity. The transmittance of the gel barely changed with increasing heating time at 50 ℃ (*Temp* > LCST), which is in associated with LCST-type gels where the turbidity is determined by the heating temperature after reaching equilibrium independent of the heating time.[10-12,16]

3.3.3 Tunable structural color by controlling the incorporated PNIPAM concentrations

Lamellar PDGI/PAAm-PNIPAM hydrogels were successfully synthesized as described as above. It should be noted that the PNIPAM concentration is important for

the thermo-sensitivity of the gel. If the PNIPAM concentration is lower or higher than 0.5 M, the color tunability with temperature is saturated. First, we investigated the lower critical solubility temperature (LCST) of PDGI/PAAm-PNIPAM hydrogels with different NIPAM concentrations through differential scanning calorimetry (DSC) (**Figure 3-6**). The formation of PNIPAM in the PDGI/PAAm hydrogel was supported by DSC results. As shown in **Figure 3-6**, the PDGI/PAAm gel shows no endothermic peak, suggesting no LCST in this temperature range. The PDGI/PAAm-PNIPAM$_{0.25M}$, PDGI/PAAm-PNIPAM$_{0.5M}$ and PDGI/PAAm-PNIPAM$_{1.0M}$ exhibited the endothermic peak around 34.9 ℃, 35.3 ℃, and 35.0 ℃, respectively. These peaks correspond to LCST of PNIPAM. These results indicates that the PNIPAM networks has been successfully incorporated into PAAm networks and the incorporation of PNIPAM networks into PAAm soft layers gives PDGI/PAAm-PNIPAM hydrogels the temperature-responsive property of PNIPAM. The incorporation of PNIPAM networks into PAAm soft layers gives PDGI/PAAm-PNIPAM hydrogels temperature-responsive property of PNIPAM with LCST around 35 ℃. The presence of the PAAm and PDGI does not appear to affect the phase separation behavior of PNIPAM in the gels.

We tuned PNIPAM density in the PDGI/PAAm-PNIPAM hydrogels by controlling the NIPAM feed concentration of the precursor solution for PNIPAM, *c*, as a parameter. We coded the obtained gels as PDGI/PAAm-PNIPAM$_{cM}$ hydrogel. Photographs of the PDGI/PAAm and PDGI/PAAm-PNIPAM hydrogels in swelling equilibrium at *Temp* = 25℃ in pure water are shown in **Figure 3-7a**. The diameter of the gels has been configured to 20 mm using a cylinder cutter. The PDGI/PAAm gels

exhibited a green structural color. The PDGI/PAAm-PNIPAM gels also exhibited bright structural color like the PDGI/PAAm gels, suggesting the periodic PDGI lamellar structure was preserved even after incorporation of PNIPAM, while their structural color was tunable by the NIPAM feed concentration, *c*. At low *c* (PDGI/PAAm-PNIPAM$_{0.25M}$), the color of the gels slightly shifted to green-orange color. With increasing *c*, the color of the gel changed to red (PDGI/PAAm-PNIPAM$_{0.5M}$) or dark-red (PDGI/PAAm-PNIPAM$_{1.0M}$). The water content of green PDGI/PAAm gel and red PDGI/PAAm-PNIPAM$_{0.5M}$ gel at 25 ºC are 90.3 and 92.0 wt%, respectively. The red shift in structural color of the PDGI/PAAm-PNIPAM gels accompanies an increase in the swelling ratio with increasing *c* (**Figure 3-7b**). Here, we observed remarkable swelling along the thickness direction but negligible swelling along the radial direction after incorporation of PNIPAM because the rigid PDGI lamellar bilayers restrict the in-plane swelling, which is discussed later in detail.[17]

The reflection spectra of the PDGI/PAAm-PNIPAM gels with diffeent *c* are shown in **Figure 3-8**. The reflection spectra showed a red shift of the reflection peak in accordance with the color shift of the gels with increasing *c*. The peak wavelength, λ_{max}, was extracted from the reflection spectra, and the distance between two lamellar layers, *d*, was estimated from λ_{max} according to Bragg's equation. As shown in **Figure 3-8b**, the λ_{max} and *d* increased linearly with increasing NIPAM concentration. The λ_{max} of PDGI/PAAm gel with green color is around 458 nm. After incorporating PNIPAM networks into PAAm soft layers, the λ_{max} increased from 458 nm to 591 nm with an increase in *c* from 0 to 1.0 M. Therefore, tuning of the structural color of PDGI/PAAm-

PNIPAM gels corresponding to a wavelength shift of 133 nm can be achieved by controlling the NIPAM concentration.

The red shift in the reflection spectrum of the PDGI/PAAm-PNIPAM gels is the result of the swelling of the gels along the thickness direction with increasing NIPAM concentration. The synthesized PNIPAM network forms an interpenetrating soft layer with PAAm in the PDGI/PAAm-PNIPAM hydrogels, which leads to an increase in osmotic pressure of the soft layers, resulting in an increased equilibrium swelling ratio of the gels.[18-20] The larger NIPAM concentration (the denser PNIPAM in the gel) leads to higher osmotic pressure, which promotes swelling more. Meanwhile, the PDGI/PAAm-PNIPAM hydrogel swells preferentially in thickness direction due to the uniaxially aligned lamellar PDGI bilayers,[21,22] which is discussed later in **Chapter 4-6**.

3.4 Summary

This chapter focuses on the strategy on incorporating PNIPAN networks into anisotropic lamellar PDGI/PAAm hydrogel to prepare thermoresponsive PNIPAM-based smart hydrogels, PDGI/PAAm-PNIPAM. The thermo-induced turbidity, tunable structural color, and anisotropic structure also has been discussed. In this chapter, we introduced the strategy for synthesizing PDGI/PAAm lamellar hydrogel and for incorporating PNIPAM networks into PAAm layers to form an interpenetrating soft layer of PAAm-PNIPAM. The resulting gel not only exhibits distinct thermo-responsive properties but also shows a red shift in structural color after incorporating.

Furthermore, the hydrogel shows tunable structural color property by controlling NIPAM concentration and the turbidity can also be tuned by controlling NIPAM concentration.

Reference

[1] M. A. Haque, G. Kamita, T. Kurokawa, K. Tsujii, J. P. Gong. Unidirectional Alignment of Lamellar Bilayer in Hydrogel: One-Dimensional Swelling, Anisotropic Modulus, and Stress/Strain Tunable Structural Color. *Adv. Mater.* **2010**, 22, 5110-5114.

[2] M. A. Haque, T. Kurokawa, G. Kamita, Y. Yue, J. P. Gong. Rapid and Reversible Tuning of Structural Color of a Hydrogel over the Entire Visible Spectrum by Mechanical Stimulation. *Chem. Mater.* **2011**, 23, 5200-5207.

[3] K. Mito, M. A. Haque, T. Nakajima, M. Uchiumi, T. Kurokawa, T. Nonoyama, J. P. Gong. Supramolecular Hydrogels with Multi-Cylindrical Lamellar Bilayers: Swelling-Induced Contraction and Anisotropic Molecular Diffusion. *Polymer* **2017**, 128, 373-378.

[4] L.Tang, L. Wang, X. Yang, Y. Feng, Y. Li, W. Feng. Poly(N-isopropylacrylamide)-Based Smart Hydrogels: Design, Properties, and Applications. *Prog. Mater. Sci.* **2021**, 115, 100702.

[5] S. A. Roget, K. A. Carter-Fenk, M. D. Fayer. Water Dynamics in Aqueous Poly-N-Isopropylacrylamide Below and Through the Lower Critical Solution Temperature. *J. Phys. Chem. B* **2022**, 126, 7066-7075.

[6] Y. Ohtsuka, M. Sakai, T. Seki, R. Ohnuki, S. Yoshioka, Y. Takeoka. Stimuli-Responsive Structural Colored Gel That Exhibits the Three Primary Colors of Light by Using Multiple Photonic Band Gaps Acquired from Photonic Balls. *ACS Appl. Mater. Interfaces* **2020**, 12, 54127-54137.

[7] F. Dalier, G. V. Dubacheva, M. Coniel, D. Zanchi, A. Galtayries, M. Piel, E. Marie, C. Tribet. Mixed Copolymer Adlayers Allowing Reversible Thermal Control of Single Cell Aspect Ratio. *ACS Appl. Mater. Interfaces* **2018**, 10, 2253-2258.

[8] W. J. Zheng, N. An, J. H. Yang, J. Zhou, Y. Chen. M. Tough Al-alginate/Poly(*N*-isopropylacrylamide) Hydrogel with Tunable LCST for Soft Robotics. *ACS Appl. Mater. Interfaces* **2015**, 7, 1758-1764.

[9] M. Radecki, J. Spěváček, A. Zhigunov, Z. Sedláková, L. Hanyková. Temperature-Induced Phase Transition in Hydrogels of Interpenetrating Networks of Poly(N-Isopropylacrylamide) and Polyacrylamide. *Eur. Polym. J.* **2015**, 68, 68-79.

[10] F. Doberenz, K. Zeng, C. Willems, K. Zhang, T. Groth. Thermoresponsive Polymers and their Biomedical Application in Tissue Engineering - A Review. *J. Mater. Chem. B* **2020**, 8, 607-628.

[11] Y. Ding, X. Zhang, B. Xua, W. Li. LCST and UCST-type Thermoresponsive Behavior in Dendronized Gelatins. *Polym. Chem.*, **2022**, 13, 2813-2821.

[12] L. Tang, L. Wang, X. Yang, Y. Feng, Y. Li, W. Feng. Poly(*N*-isopropylacrylamide)-Based Smart Hydrogels: Design, Properties and Applications. *Prog. Mater. Sci.* **2021**, 115, 100702.

[13] Y. S. Kim, M. Liu, Y. Ishida, Y. Ebina, M. Osada, T. Sasaki, T. Hikima, M. Takata and T. Aida Thermoresponsive Actuation Enabled by Permittivity Switching in an Electrostatically Anisotropic Hydrogel. *Nat. Mater.* **2015**, 14, 1002-1007.

[14] S. A. Roget, K. A. Carter-Fenk, M. D. Fayer Water Dynamics in Aqueous Poly-N-Isopropylacrylamide Below and Through the Lower Critical Solution Temperature. *J. Phys. Chem. B* **2022**, 126, 7066-7075.

[15] Y. Ohtsuka, M. Sakai, T. Seki, R. Ohnuki, S. Yoshioka, Y. Takeoka. Stimuli-Responsive Structural Colored Gel That Exhibits the Three Primary Colors of Light by Using Multiple Photonic Band Gaps Acquired from Photonic Balls. *ACS Appl. Mater. Interfaces* **2020**, 12, 54127-54137.

[16] C. Yu, K. Cui, H. Guo, Y. N. Ye, X. Li, J. P. Gong. Structure Frustration Enables Thermal History-Dependent Responsive Behavior in Self-Healing Hydrogels. *Macromolecules* **2021**, 54, 9927-9936.

[17] Y. F. Yue, M. A. Haque, T. Kurokawa, T. Nakajima, J. P. Gong. Lamellar Hydrogels with High Toughness and Ternary Tunable Photonic Stop-Band. *Adv. Mater.* **2013**, 25, 3106-3110.

[18] H. Na, Y-W. Kang, C. S. Park, S. Jung, H-Y. Kim, J-Y. Sun. Hydrogel-Based Strong and Fast Actuators by Electroosmotic Turgor Pressure. *Science* **2022**, 376, 301-307.

[19] X. Li, X. Cai, Y. Gao, M. J. Serpe. Reversible Bidirectional Bending of Hydrogel-Based Bilayer Actuators. *J. Mater. Chem. B* **2017**, 5, 2804-2812.

[20] M. E. Harmon, M. Tang, C. W. Frank. A Microfluidic Actuator Based on Thermoresponsive Hydrogels. *Polymer* **2003**, 44, 4547-4556.

[21] Y. F. Yue, M. A. Haque, T. Kurokawa, T. Nakajima, J. P. Gong. Lamellar Hydrogels with High Toughness and Ternary Tunable Photonic Stop-Band. *Adv. Mater.* **2013**, 25, 3106-3110.

[22] M. A. Haque, K. Mito, T. Kurokawa, T. Nakajima, T. Nonoyama, M. Ilyas, J. P. Gong. Tough and Variable-Band-Gap Photonic Hydrogel Displaying Programmable Angle-Dependent Colors. *ACS Omega* **2018**, 3, 55-62.

Dodecyl Glyceryl Itanonate (DGI)

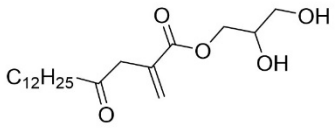

Acrylamide (AAm)

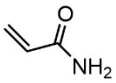

Irgacure 2959

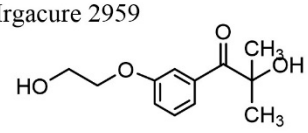

N,N'-Methylenebisacrylamide (MBAA)

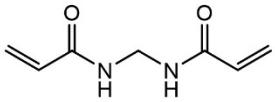

Sodium Dodecyl sulfate (SDS)

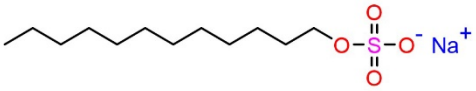

N-isopropylacrylamide (NIPAM)

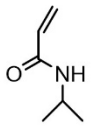

Figure 3-1. Molecular formula of DGI, AAm, Irgacure 2959, MBAA, SDS, NIPAM in this work.

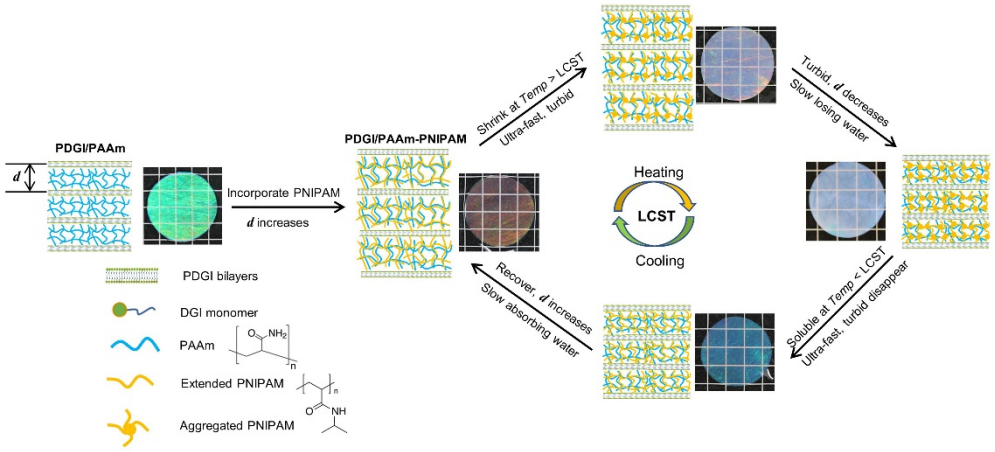

Figure 3-2. Illustration of the thermo-responsive anisotropic photonic hydrogel, PDGI/PAAm-PNIPAM hydrogel. This hybrid hydrogel has a hard, anisotropic PDGI bilayer and a soft, thermo-responsive PAAm-PNIPAM layer. When the temperature (*Temp*) is higher than the lower critical solution temperature (LCST) of PNIPAM, the PNIPAM network becomes hydrophobic, and the gel becomes turbid immediately and releases water gradually. With the water release, the gel mainly shrinks along the thickness direction owing to the presence of macroscopic bilayers, and the interplanar distance of the gel decreases gradually, leading change in the structural color. At *Temp* < LCST, PNIPAM becomes hydrophilic and the turbidity disappears immediately. The interplanar distance of the gel increases gradually absorbing water to reach the original/swollen state.

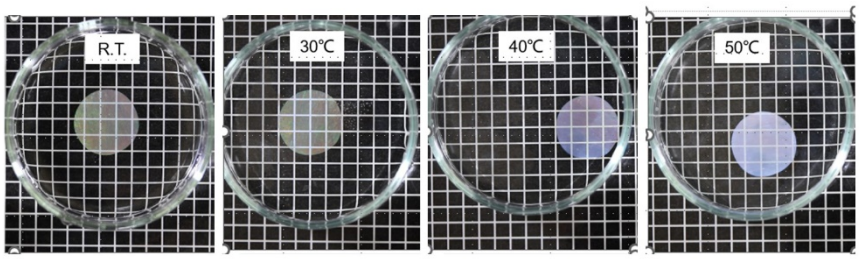

Figure 3-3: Photographs of PDGI/PAAm-PNIPAM$_{0.5M}$ in pure water at different temperatures. Background lattices: 5 × 5 mm.

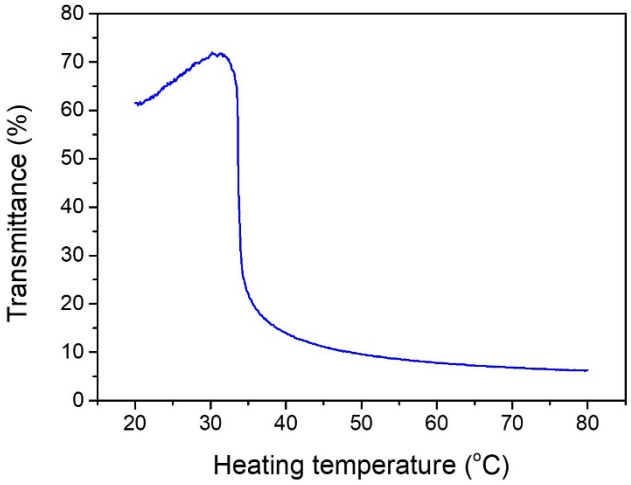

Figure 3-4: Transmittance of the PDGI/PAAm-PNIPAM$_{0.5M}$ gel at 400 nm during heating at a heating rate of 1.0 ℃/min. The gel was initially equilibrated in water at 20 ℃ for 1 h before measurement and then heated from 20 to 80 ℃.

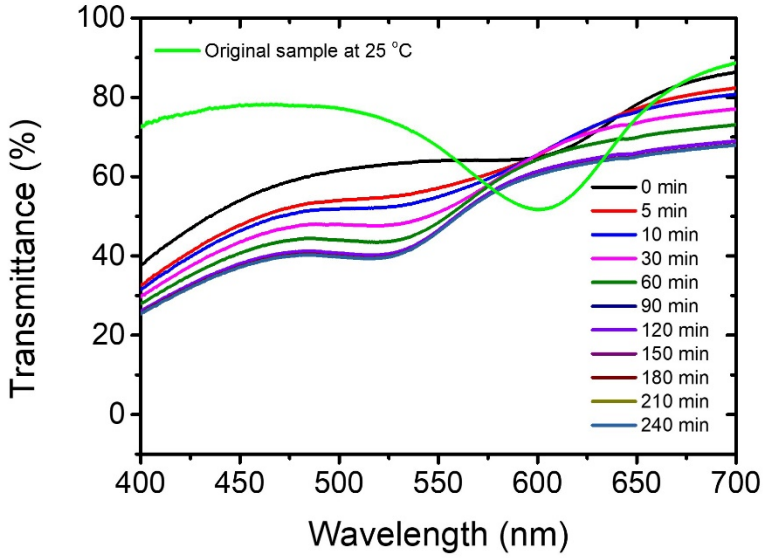

Figure 3-5: Transmittance of PDGI/PAAm-PNIPAM$_{0.5M}$ gels during heating process at 50 ℃.

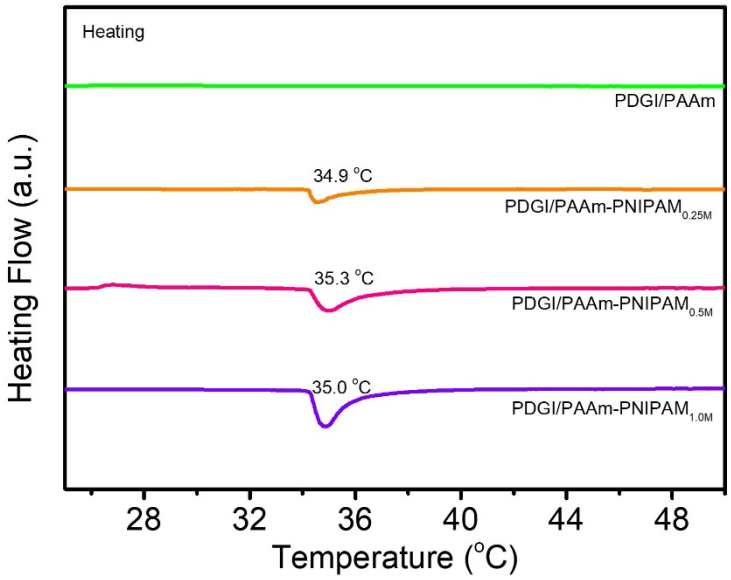

Figure 3-6: DSC thermograms of PDGI/PAAm and PDGI/PAAm-PNIPAM gels with different NIPAM concentrations.

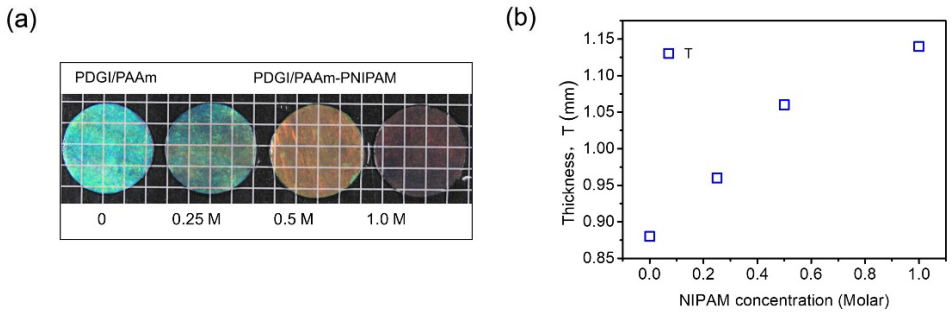

Figure 3-7: (a) Photographs and (b) thickness, T, of PDGI/PAAm and PDGI/PAAm-PNIPAM hydrogels synthesized with different NIPAM feed concentrations in pure water at room temperature. Background lattices: 5 × 5 mm.

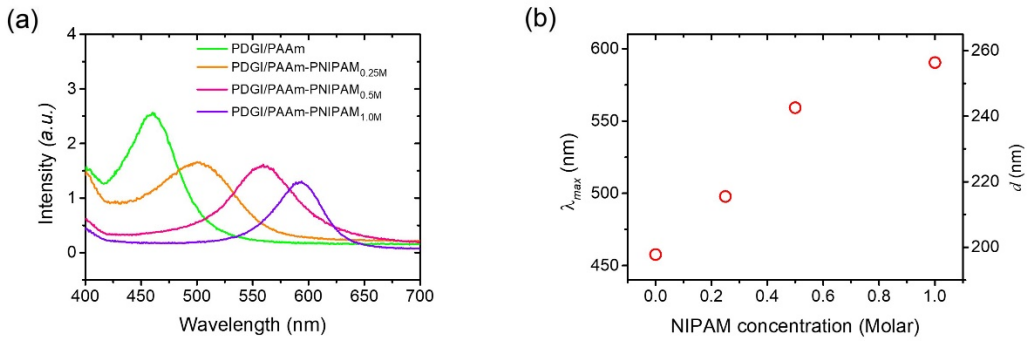

Figure 3-8: (a) Reflection spectra of PDGI/PAAm and PDGI/PAAm-PNIPAM hydrogels synthesized with different NIPAM feed concentration in pure water at room temperature; (b) Peak wavelength, λ_{max}, of the reflection spectrum and the corresponding interplanar distance, *d*, as a function of NIPAM concentration.

Chapter 4: Swelling behavior of thermo-responsive lamellar hydrogel

4.1 Introduction

Hydrogels, remarkable polymeric materials abundant in water content, offer immense potential as biomaterials in tissue engineering. Nevertheless, a prevalent limitation lies in the isotropic structures of the majority of hydrogels, both at microscopic and macroscopic scales.[1] This arises from their common synthesis method, wherein monomers dissolved in water undergo photo or thermal polymerization, leading to a lack of molecular orientation. Conventional hydrogel materials with unordered homogeneous structures inevitably lack high mechanical properties and anisotropic functional performances; thus, their further application is limited. Inspired by biological soft tissues with well-ordered structures, researchers have increasingly investigated highly ordered nanocomposite hydrogels as functional biological engineering soft materials with unique mechanical, optical, and biological properties.[2,3] These hydrogels incorporate long-range ordered nanocomposite structures within hydrogel network matrixes.

The development of a cohesive anisotropic structure at the macroscopic scale in hydrogels remains a complex and formidable undertaking. These anisotropic hydrogels with highly ordered structures have attracted enormous attention.[1-5] The ordered structure of the hydrogels imparts excellent anisotropic functions and makes them promising candidates for applications in sensors, soft robotics, artificial muscles, and

biological engineering, owing to their soft and wet nature.[2] Therefore, highly ordered nanocomposite structures need to be introduced into hydrogel networks to obtain superb anisotropic functions for biological engineering applications. It is of great importance to propose more advanced and effective strategies of fabricating hydrogels with highly ordered structures and anisotropic performances.[6-8]

Thermo-responsive polymers, exemplified by poly-*N*-isopropylacrylamide (PNIPAM), polyvinylpyrrolidone (PVP), and poly *N*,*N*-diethylacrylamide (PDEAAm), exhibit a distinctive behavior of shrinking or expanding in response to temperature changes.[9] Of particular interest is NIPAM due to its lower critical solution temperature (LCST), which aligns closely with the human body temperature, approximately 32°C.[9-12]

PNIPAM stands out for its reversible and conspicuous volume alterations in the vicinity of its LCST. This characteristic makes it a compelling and extensively studied material in the realm of temperature-sensitive smart polymers. Researchers are drawn to its potential applications in various fields, particularly in biomedical and drug delivery systems, where the ability to respond to the physiological temperature of the human body is crucial.[12]

The capacity of PNIPAM and similar smart polymers to undergo reversible changes in volume at specific temperature thresholds opens avenues for designing responsive materials with tailored properties.[9-13] The exploration of these polymers not only contributes to advancements in fundamental polymer science but also holds promise for practical applications in developing innovative materials with controlled

responses to temperature stimuli. As such, the research focus on PNIPAM-based anisotropic hydrogels continue to drive progress in the development of intelligent materials with diverse applications in biotechnology, nanotechnology, and beyond.[13,14]Departing from conventional thermo-responsive hydrogels, the incorporation of thermo-responsive polymers into anisotropic hydrogels or structure-directing templates such as 2-D materials hold the potential to introduce unique functionalities and properties. These innovations, stemming from the synergy of thermo-responsiveness and anisotropic structures, could open up a new chapter in material science.

4.2 Experiments

4.2.1 Materials

DGI was synthesized and purified according to our previous work.[15] The DGI fraction was eluted with a hexane/ethyl acetate mixture (1:1 by volume) and was further purified twice by recrystallization from an acetone/hexane mixture (1/1 by weight). *N*,*N*′-methylenebis(acrylamide) (MBAA, 99.0%, FUJIFILM Wako Pure Chemical Corporation, Japan) was recrystallized from ethanol, acrylamide (AAm, 98%, JUNSEI Chemicals Co. Ltd., Japan) was recrystallized from chloroform, *N*-isopropylacrylamide (NIPAM, 97%, Sigma-Aldrich Co., USA) was recrystallized twice from an ether/hexane mixture. 2-Hydroxy-4′-(2-hydroxyethoxy)-2-methylpropiophenone (Irgacure 2959, 98%, Sigma-Aldrich Co., USA) and sodium dodecyl sulfate (SDS, 98%, FUJIFILM Wako Pure Chemical Corporation, Japan) were used as received. Milli-Q

deionized water was used to prepare the monomer solutions and for the swelling of the gel.

4.2.2 Preparation of PAAm-PNIPAM double network hydrogels

A PAAm-PNIPAM interpenetrating network gel without PDGI bilayers was prepared by incorporating the PNIPAM into the PAAm network. The PAAm network was synthesized by 4 M AAm, 4 mM MBAA as a cross-linker of AAm, and 2 mM Irgacure 2959 as an initiator. The incorporation of the PNIPAM network follows the same way as mentioned in Chaptr 3.

4.2.3 Polarized optical microscope observation

The anisotropic structure of gels was observed by the polarized optical microscope (POM, Nikon Eclipse LV100POL) under crossed Nicol at 25°C. A tint plate (530 nm) was used to examine the orientation direction. The observation was performed from the top surface (top view) and the cross-section (side view) of the sheet-like gels. Before the observation, the gel sample was cut into a rectangular sheet (~50 x 2 x 1.2 mm^3 for the top view and ~30 x 1 x 1.2 mm^3 for the side view). POM images of the fully swollen PDGI/PAAm and PDGI/PAAm-$PNIPAM_{0.5M}$ hydrogels in water at *Temp* = 25°C were shown in **Figure 4-1**.

4.2.4 Reflection spectrum

Reflection spectra of various gel samples were measured by a combined setup of a light source, variable angle measurement device, and an analyzer. An Xe lamp was

used as a light source to obtain the reflection spectrum. Reflection measurement optics with variable angles (Hamamatsu Photonics KK, C10027A10687) were used to detect the reflected light. A photonic multichannel analyzer (Hamamatsu Photonics KK, C10027) was used for analyzing the detected signals. The entire reflection spectrum was obtained by keeping the incident angle at 60° and reflection angles at 45°. The distance between two lamellar layers, *d*, was roughly calculated using Bragg's law of diffraction, $\lambda_{max} = 2nd\sin\theta$, where $n = 1.33$ is the refractive index of water, θ is the incident angle, and λ_{max} is the wavelength at maximum reflectance intensity.[15-17] The reflection spectra of the PDGI/PAAm and PDGI/PAAm-PNIPAM$_{0.5M}$ gel during heating and cooling process around LCST were measured and compared as shown in **Figure 4-2**.

4.2.5 Swelling Ratio Measurement

For the swelling experiment, a swollen gel was cut into a cylindrical shape using a cylinder cutter (Diameter = 20.0 mm). The diameter of a cylindrical gel at different swollen states, *D*, was measured by a slide caliper. The thickness of the PDGI/PAAm and PDGI/PAAm-PNIPAM gels, *T*, was measured using a mechanical thickness meter (Teclck, Dumb Bell Ltd., Japan), and the thickness of the PAAm-PNIPAM gels was measured by Keyence laser thickness mater (CL-L015N, Keyence Corporation, Japan).

4.2.6 Water content measurement

The water content of the gel was measured using a moisture balance MOC-120H (Shimadzu Co.). The wet sample was obtained by heating the sample to 120 °C. The

water content of green PDGI/PAAm and red PDGI/PAAm-PNIPAM$_{0.5M}$ gel at 25 ºC are 90.3 and 92.0 wt%, respectively. The water content of blue PDGI/PAAm-PNIPAM$_{0.5M}$ gel after reach new equilibrium at 50 ºC is 87.9 wt%. The notable decrease in water content of PDGI/PAAm-PNIPAM$_{0.5M}$ gel at 50 ºC, which is indicative of water releasing along with a decrease in the *d*-value, is attributed to the phase separation of the PNIPAM networks at temperature > 33 ºC, which is its lower critical solution temperature (LCST).

4.3 Results and Discussion

4.3.1 Structure of thermo-responsive lamellar hydrogel

Polarizing optical microscopy (POM) images were captured to justify the structural anisotropy of the PDGI/PAAm and PDGI/PAAm-PNIPAM$_{0.5M}$ lamellar hydrogels swollen in water at *Temp* = 25 °C (**Figure 4-1**). The sample setup and observation directions are shown in the Figure. All the images were taken under cross-polarizers in the presence of a tint plate (530 nm). The PDGI/PAAm hydrogel exhibited strong birefringence, which has been assigned to the aligned monodomain bilayers and elongated PAAm chains along the direction perpendicular to the PDGI bilayers on account of the anisotropic swelling.[18] The PDGI/PAAm-PNIPAM$_{0.5M}$ gel with the incorporated PNIPAM network also exhibited strong birefringence. As shown in **Figure 4-1a(i-iii)** and **4-1b(i-iii)**, images of the cross-section of the PDGI/PAAm and PDGI/PAAm-PNIPAM$_{0.5M}$ lamellar gel (side) appeared orange at −45°(i), magenta at 0° (ii), and blue at +45°(iii) rotations relative to the polarizer, respectively. These results

indicate that incorporating PNIPAM networks into PAAm layers does not affect the anisotropic swelling behavior along the thickness direction of the lamellar hydrogel. The monodomain PDGI bilayers in the gel, which govern the swelling anisotropy, barely got damaged after incorporating 0.5 M PNIPAM networks into PAAm layers, corresponding to the highly anisotropic swelling behaviors.

Top-view POM images of these lamellar gels showed no birefringence color at any rotation angle, confirming the isotropic in-plane structure of the lamellar bilayers (**Figure 4-1a, b(iv-vi)**).

4.3.2 Thermo-induced ultrafast structural color/turbid transition

The unique properties of PDGI/PAAm-PNIPAM hydrogels derived from their thermo-responsibility and anisotropic structure were discussed in this section. The obtained PDGI/PAAm-PNIPAM gels exhibit unique temperature-responsive visual and size change. As the typical example, results of the PDGI/PAAm-PNIPAM$_{0.5M}$ gel as the model gel are shown here.

As discussed in **Chapter 3**, the PDGI/PAAm-PNIPAM lamellar hydrogel shows the thermo-induced ultra-fast turbid/transparent transition phenomenon of the PDGI/PAAm-PNIPAM$_{0.5M}$ hydrogels (diameter = 20 mm, thickness ~ 1.0 mm) during heating and cooling process around LCST. The gel exhibited structural color at 25°C but instantly turned turbid when immersed into the 50 °C hot water bath owing to hydrophobic association of the PNIPAM chains in the gel. It is worth mentioning that the turbidity of the heated gel is controllable by the heating temperature above LCST

(**Chapter 3**).[11-14] When the heated gel was suddenly cooled to 25 ℃, the turbidity disappeared immediately due to the recovery of hydrophilicity of the PNIPAM chains.[11-14] Timescale of the transparent/turbid transition was ~1 s. Note that ultrafast transparent/turbid transition of the aqueous PNIPAM-based smart materials is general. Unlike typical smart materials, which are colorless at low temperature,[9] in this work, we utilized the hydrogels with bright structural color as the base material to realize structure color/turbid transition. The colorful gels immediately turn into monochrome gels just by heating, which could be called the thermo-induced color/monochrome transition.

The long-term thermo-responsive behaviors of the PDGI/PAAm-PNIPAM$_{0.5M}$ hydrogels during the heating and cooling process across LCST were then investigated, including gradual structural color change and anisotropic deswelling/reswelling. The experimental process was shown in **Figure 4-2**. The PDGI/PAAm-PNIPAM$_{0.5M}$ hydrogel at swelling equilibrium in a 25 ℃ cold water bath showed a red color. The red gel was then immersed into 50 ℃ hot water bath for the time t_1. Pictures of the gels being heated at 50 ℃ for varied t_1 is shown in **Figure 4-3(A)**. The turbidity of the gel does not decay with time during heating (**Figure 4-3(A)** and **Figure 3-5**), which is in accord with the LCST-type gels where the turbidity is mainly determined by the temperature but independent of time.[11-14] On the other hand, diameter and the hidden structural color of the gels seem to change with t_1. In contrast to the constant turbidity, the gel gradually expelled water with t due to the hydrophobicity of PNIPAM.

Deswelling of the lamellar gels leads change of their structure color hidden by the turbidity. Although the PDGI/PAAm-PNIPAM$_{0.5M}$ hydrogel was turbid at 50 ℃, it seems to exhibit faint structural color hidden by the turbidity. To investigate the hidden structural color of the PDGI/PAAm-PNIPAM$_{0.5M}$ gel during heating, the gel heated for the desired time t_1 was quenched by immersion into a 25 ℃ cold water bath. After immediate disappearance of the turbidity of the gel, the instantaneous structural color of the gel was captured immediately. After immediate disappear of the turbidity of the gel, the instantaneous structural color of the gel was captured immediately. The quenched gel showed a t_1-dependent blue shift in the structural color (**Figure 4-3(A')**). The color of the quenched gel gradually changed from red to green with the increase of t_1. At $t_1 > 2$ h, the gel showed no further structural color change.

The reflection spectra also show a blue shift in peak wavelength, λ_{max}, from higher (~548 nm) to lower (~465 nm) wavelength in accordance with the blue shift in color with the increase of t_1 (**Figure 4-4** and **4-5**). This indicates that the gel reached the new equilibrium state at 50 ℃ after 2 h heating at this condition. It should be noticed that bluish color was glimpsed in the turbid gel (**Figure 4-3(A)**) independent of its hidden structural color (**Figure 4-3(A')**). This is probably due to Rayleigh and Mie scatterings of aggregated PNIPAM in the gel. During heating at *Temp* > LCST, the PNIPAM polymer chains within the networks undergo collapse and aggregation, leading to the formation of micro- or nanoscale structures that scatter light according to Rayleigh and Mie scattering theories.[19]

We immersed the gel equilibrated at 50 ℃ into 25 ℃ cold water bath for the reswelling time t_2 and obtained the reflection spectra and corresponding d. When the quenched gel was continuously immersed in 25 ℃ cold water bath, the gel gradually recovers the original color (**Figure 4-3(B)**) as well as the original λ_{max} (~548 nm) and d (~ 237 nm) with the reswelling time t_2 (**Figure 4-4** and **4-5**). λ_{max} and d decrease/increase accordingly during the heating/cooling processes. Figure 4-3(B) and Figure 4-4 show the change of d and the reflection spectra of the gel, respectively, with different reswelling times t_2. The increase in d during recovery is on account of the reswelling of the PAAm-PNIPAM soft layer at $Temp$ < LCST.[9] This indicates that the thermal-induced structural color change of the gel is reversible.

4.3.3 Thermo-induced anisotropic deswelling/reswelling

We also measured the thermo-induced anisotropic deswelling/swelling of the gel during the heating and reswelling process (**Figure 4-6**). Here, we set the PDGI/PAAm-$PNIPAM_{0.5M}$ hydrogel swollen in 25 ℃ cold water as the reference state, and the diameter and thickness of the gel at this state were set as D_0 and T_0. The gel was then heated at $Temp$ = 50 ℃ for t_1. The diameter and thickness of the gel at this stage are shown as $D_1(t_1)$ and $T_1(t_1)$, and those at new shrunken equilibrium state are shown as D_1 and T_1. The gel at new shrunken equilibrium state was then quenched and kept in 25 ℃ cold water for t_2 to reswell. The diameter and thickness of the gel at reswelling time t_2 are shown as $D_2(t)$ and $T_2(t)$, and at fully recovered state as D_2 and T_2, respectively. The deswelling ratio of the cylindrical gel in the thickness direction

(perpendicular to PDGI bilayer) and diameter direction (parallel to PDGI bilayer) were defined as $T_1(t_1)/T_0$ and $D_1(t_1)/D_0$, respectively. Similarly, the reswelling ratio of the gel in the thickness and diameter directions are $T_2(t_2)/T_1$ and $D_2(t_2)/D_1$, respectively. Since the PDGI lipid bilayers in the PDGI/PAAm hydrogels are almost water impermeable and without any in-plane anisotropy,[15-18] the thermal-induced deswelling/reswelling of the gel is considered to only occur in the PAAm-PNIPAM soft layers. As shown in **Figure 4-6**, the deswelling ratio of the PDGI/PAAm-PNIPAM$_{0.5M}$ gel in the thickness direction ($T_1(t_1)/T_0$) decreases down to 0.85 with increasing heating time t_1. On the other hand, only slight decrease ($D_1(t_1)/D_0 \sim 0.95$) in the diameter direction is observed. For the cooling process, the gel fully recovered its original size ($T_2/T_1 \approx 1.15 > D_2/D_1 \approx 1.04$) after 2 h immersion in 25°C cold water, as observed from the photographs of the gel. These indicate that the PDGI/PAAm-PNIPAM hydrogel shows reversible thermal-induced deswelling/reswelling behaviors significant anisotropy.

The PAAm-PNIPAM soft layers in PDGI/PAAm-PNIPAM gels mainly shrink/swell perpendicular to the bilayer direction under thermal stimuli, in contrast to isotropic deswelling/reswelling of typical PNIPAM-based hydrogels. For example, the PAAm-PNIPAM$_{0.5M}$ isotropic interpenetrating hydrogel without PDGI bilayer does not exhibit such swelling anisotropy during heating and cooling process (**Figure 4-7**). Since PDGI lipid bilayers can be deemed as unexpandable stiff sheets, in-plain swelling/deswelling of the gel is restricted because such swelling must accompany expansion of stiff sheets. This causes anisotropic deswelling of the gel along the thickness direction and the a remarkable decrease in the interplanar distance as well as

blue shift of the structural color of the gel upon heating.[15-18] The details can be seen from the following discussion.

4.3.4 Deswelling/reswelling behaviors of PAAm-PNIPAM gels

The visual change and deswelling/reswelling behaviors of PAAm-PNIPAM$_{0.5M}$ double networks hydrogels (diameter ≈ 20 mm, thickness ~ 1.0 mm) during heating and cooling process around LCST was shown in **Figure 4-7**. The original PAAm-PNIPAM$_{0.5M}$ gel at the 25 ℃ water bath was transparent (**Figure 4-7a, left**). The gel was transferred into 50 ℃ hot water bath for desired time, t_1 (**Figure 4-7a, up**). The gel turns to turbid instantly when immersed into the 50 ℃ hot water bath owing to hydrophobic association of the PNIPAM chains in the gel, and the turbidity of the gel does not decay with time during heating. After a 4 h heating process, the heated (deswollen) gel was cooled to 25 ℃ for desired time, t_2 (**Figure 4-7a, down**). The turbidity disappears immediately and the gel becomes transparent because the PNIPAM chains return to hydrophilic.

The PAAm-PNIPAM$_{0.5M}$ gel shows isotropic deswelling/reswelling behaviors during the heating and cooling process around LCST, as shown in **Figure 4-7b** and **Figure 4-7c**. The diameter of the gel decreased during the heating process before reaching equilibrium. The deswelling ratio of the gel during heating process is shown in **Figure 4-7b**. As can be seen, the deswelling ratio of the PAAm-PNIPAM$_{0.5M}$ gel in the thickness direction (T_1/T_0) and the diameter direction (D_1/D_0) both decreases down to ~ 0.78 with increasing heating time. In addition, the gel fully recovers to the original

size ($T_2/T_1 \approx D_2/D_1 \approx 1.35$) after the cooling process, as observed from the photographs of the gel (**Figure 4-7c**). This indicates that the PAAm-PNIPAM gel shows reversible and isotropic deswelling/reswelling behaviors.

4.3.5 Time difference for structural color/turbid phenomenon (<1 s) and swelling process (~2 h)

The time difference for ultrafast structural color/turbid phenomenon (<1 s) and swelling process (~2 h) is discussed. An illustration to explain the cause of the difference is shown in **Figure 4-8**. The original PDGI/PAAm-PNIPAM$_{0.5M}$ hydrogel turns turbid immediately after immersing into hot water and the turbidity disappears immediately after quenching the gel into cold water. This is because the PNIPAM-based lamellar gel exhibits immediate microphase separation same as typical PNIPAM aqueous systems at *Temp* > LCST.[9] Once the gel is immersed into hot water, the PNIPAM network instantly becomes hydrophobic and aggregate together, resulting in the turbidity of the gel. Such hydrophobicity of PNIPAM also causes deswelling of the gel. Since deswelling requires long-path diffusion of water molecules, the timescale of diffusion of water for deswelling is much longer than that of the phase separation. In the case of the gels with the water impermeable monodomain PDGI bilayers, the diffusion of water into and out of the hydrogel occurs mainly along the diameter direction. In short, the PDGI/PAAm-PNIPAM hydrogels show anisotropic diffusion. Timescale of water diffusion in the gel along this path can be estimated by the equation for 2-D diffusion, $t = L^2/4d_w$, where t is diffusion timescale, L is length of the diffusion

path, and D_w is diffusion coefficient of water.[20,21] We roughly assume that D_w in the PDGI/PAAm-PNIPAM gel is the same as that of free water. By substitution of L = 1 cm (radius of the cylindrical gel) and $D_w = 3.983\times10^{-5}$ cm^2 s^{-1} at 50 ℃, the timescale of deswelling (t_{ds}) becomes 1.74 h. It indicates that the time for PDGI/PAAm-PNIPAM$_{0.5M}$ hydrogel to reach shrunken equilibrium at 50 ℃ is 1.74 h. While that for reswelling at 25 ℃, $D_w = 2.299\times10^{-5}$ cm^2 s^{-1}.[20] Therefore, the timescale of reswelling (t_{rs}) for the shrunken hydrogel to recover original state becomes 3.02 h. These estimations are in agreement with the experimentally observed deswelling/reswelling timescales.

4.4 Conclusion

In this chapter, we prepared PDGI/PAAm-PNIPAM hydrogels. The hydrogel still exhibits anisotropic lamellar structure. We can facilely tune the turbidity of the photonic PDGI/PAAm-PNIPAM hydrogels with temperature, leading the structure color/turbid transition of the gel at LCST. Moreover, since dehydrolyzation of PNIPAM in a gel at high temperature also leads deswelling of a whole gel, deswelling/reswelling ratio of the PDGI/PAAm-PNIPAM hydrogels can also be tuned by the temperature, leading tunable structural color and anisotropic deswelling/reswelling by temperature stimuli around LCST. In short summary, the PDGI/PAAm-PNIPAM hydrogels exhibit ultrafast structural color/turbid transition, gradual structural color change, and anisotropic swelling upon heating and cooling processes. In the following sections, we investigate each thermal-responsive phenomenon of the gels in detail.

Reference

[1] Y. Yue, J. P. Gong. Structure and Unique Functions of Anisotropic Hydrogels Comprising Uniaxially Aligned Lamellar Bilayers. *Bull. Chem. Soc. Jpn.* **2021**, *94*, 2221-2234.

[2] Z. Zhao, R. Fang, Q. Rong, M. Liu. Bioinspired Nanocomposite Hydrogels with Highly Ordered Structures. *Adv. Mater.* **2017**, 29, 1703045.

[3] H. Arslan, A. Nojoomi, J. Jeon, K. Yum. 3D Printing of Anisotropic Hydrogels with Bioinspired Motion. *Adv. Sci.* **2019**, 6, 1800703.

[4] K. Sano, Y. Ishida, T. Aida. Synthesis of Anisotropic Hydrogels and Their Applications. *Angew. Chem. Int. Ed.* **2018**, 57,2532-2543.

[5] K. Sano, Y. Ishida, T. Aida. Synthesis of Anisotropic Hydrogels and Their Applications. *Angew. Chem. Int. Ed.* **2018**, 57,2532-2543.

[6] N. Miyamoto, M. Shintate, S. Ikeda, Y. Hoshida, Y. Yamauchi, R. Motokawa, M. Annaka. Liquid Crystalline Inorganic Nanosheets for Facile Synthesis of Polymer Hydrogels with Anisotropies in Structure, Pptical Property, Swelling/Deswelling, and Ion Transport/Fixation. *Chem. Commun.* **2013**, 49, 1082-1084.

[7] C. Zhao, P. Zhang, J. Zhou, S. Qi, Y. Yamauchi, R. Shi, R. Fang, Y. Ishida, S. Wang, A. P. Tomsia, M. Liu, L. Jiang. Layered Nanocomposites by Shear-Flow-Induced Alignment of Nanosheets. *Nature* **2020**, 580, 210-215.

[8] C. Xing, S. Chen, X. Liang, Q. Liu, M. Qu, Q. Zou, J. Li, H. Tan, L. Liu, D. Fan, H. Zhang. Two-Dimensional MXene ($Ti_3C_{(2)}$)-Integrated Cellulose Hydrogels: Toward Smart Three-Dimensional Network Nanoplatforms Exhibiting Light-Induced Swelling and Bimodal Photothermal/Chemotherapy Anticancer Activity. *ACS Appl. Mater. Interfaces* **2018**, 10, 27631-27643.

[9] L. Tang, L. Wang, X. Yang, Y. Feng, Y. Li, W. Feng. Poly(*N*-isopropylacrylamide)-based Smart Hydrogels: Design, Properties and Applications. *Prog. Mater. Sci.* **2021**, 115, 100702.

[10] Y. S. Kim, M. Liu, Y. Ishida, Y. Ebina, M. Osada, T. Sasaki, T. Hikima, M. Takata,

T. Aida. Thermoresponsive Actuation Enabled by Permittivity Switching in An Electrostatically Anisotropic Hydrogel. *Nat. Mater.* **2015**, 14, 1002-1007.

[11] Z. Ye, S. Sun, P. Wu. Distinct Cation-Anion Interactions in the UCST and LCST Behavior of Polyelectrolyte Complex Aqueous Solutions. *ACS Macro Lett.* **2020**, 9, 974-979.

[12] F. Doberenz, K. Zeng, C. Willems, K. Zhang, T. Groth. Thermoresponsive Polymers and Their Biomedical Application in Tissue Engineering - A Review. *J Mater. Chem. B* **2020**, 8, 607-628.

[13] A. Asadujjaman, B. Kent, A. Bertin. Phase Transition and Aggregation Behaviour of an UCST-Type Copolymer Poly-(Acrylamide-Co-Acrylonitrile) in Water: Effect of Acrylonitrile Content, Concentration in Solution, Copolymer Chain Length and Presence of Electrolyte. *Soft Matter* **2017**, 13, 658-669.

[14] J. Li, Q. Ma, Y. Xu, M. Yang, Q. Wu, F. Wang, P. Sun. Highly Bidirectional Bendable Actuator Engineered by LCST-UCST Bilayer Hydrogel with Enhanced Interface. *ACS Appl. Mater. Interfaces* **2020**, 12, 55290-55298.

[15] M. A. Haque, G. Kamita, T. Kurokawa, K. Tsujii, J. P. Gong. Unidirectional Alignment of Lamellar Bilayer in Hydrogel: One-Dimensional Swelling, Anisotropic Modulus, and Stress/Strain Tunable Structural Color. *Adv. Mater.* **2010**, 22, 5110-5114.

[16] M. A. Haque, T. Kurokawa, G. Kamita, Y. Yue, J. P. Gong. Rapid and Reversible Tuning of Structural Color of a Hydrogel over the Entire Visible Spectrum by Mechanical Stimulation. *Chem. Mater.* **2011**, 23, 5200-5207.

[17] M. A. Haque, T. Kurokawa, T. Nakajima, G. Kamita, Z. Fatema, J. P. Gong. Surfactant Induced Bilayer-Micelle Transition for Emergence of Functions in Anisotropic Hydrogel. *J. Mater. Chem. B* **2022**, 10, 8386-8397.

[18] M. A. Haque, K. Mito, T. Kurokawa, T. Nakajima, T. Nonoyama, M. Ilyas, J. P. Gong. Tough and Variable-Band-Gap Photonic Hydrogel Displaying Programmable Angle-Dependent Colors. *ACS Omega* **2018**, 3, 55-62.

[19] Y. Ding, Y. Duan, F. Yang, Y. Xiong, S. Guo. High-Transmittance PNIPAm Gel Smart Windows with Lower Response Temperature and Stronger Solar Regulation. *Chem. Eng. J.* **2023**, 460, 141572.

[20] Holz, M.; Heil, S. R.; Sacco, A. Temperature-Dependent Self-Diffusion Coefficients of Water and Six Selected Molecular Liquids for Calibration in Accurate ^{1}H NMRPFG Measurements. *Phys. Chem. Chem. Phys.* **2000**, 2, 4740-4742.

[21] Cui, K.; Yu, C.; Ye, Y. N.; Li, X.; Gong, J. P. Mechanism of Temperature-Induced Asymmetric Swelling and Shrinking Kinetics in Self-Healing Hydrogels. *PNAS* **2022**,119, e2207422119.

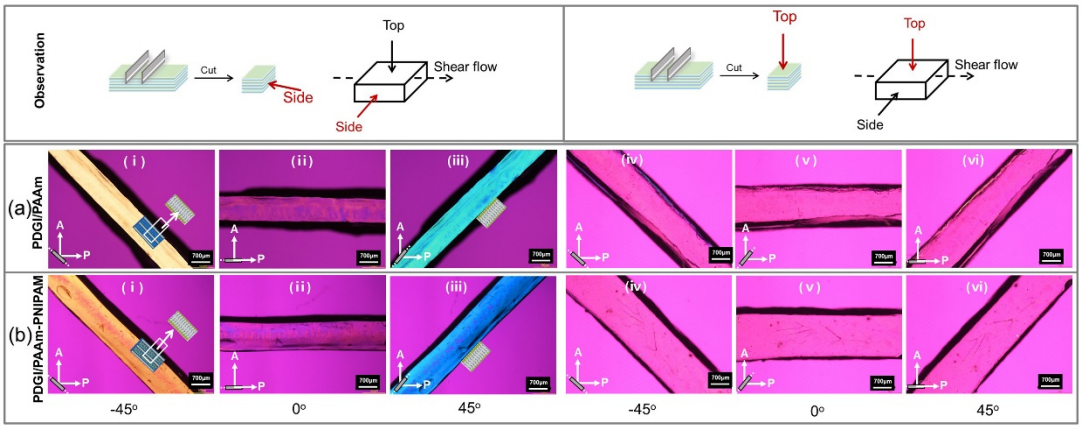

Figure 4-1: Polarizing optical microscope (POM) images of (a) PDGI/PAAm and (b) PDGI/PAAm-PNIPAM$_{0.5M}$ gels. The sample setup and observation directions are also shown. All the images are taken under cross-polarizers in the presence of a tint plate (530 nm). The scale bars are 700 μm.

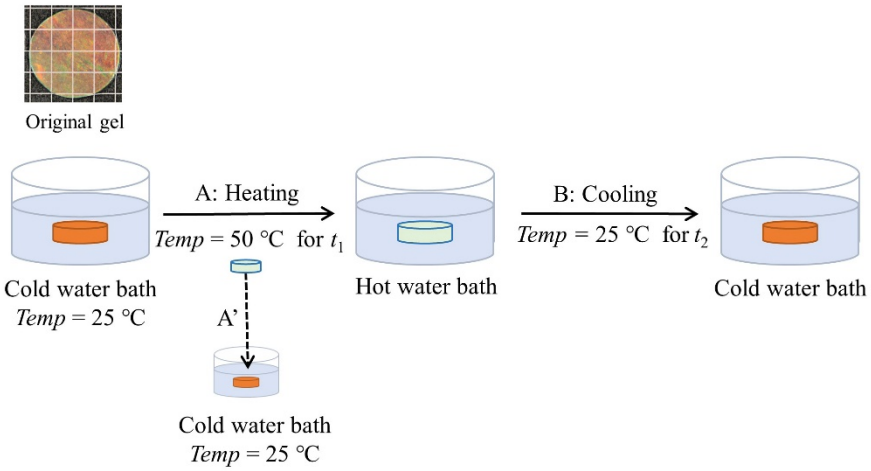

Figure 4-2: Experimental illustration for heating (for desired t_1) and cooling (for desired t_2) process of PDGI/PAAm-PNIPAM$_{0.5M}$ gel.

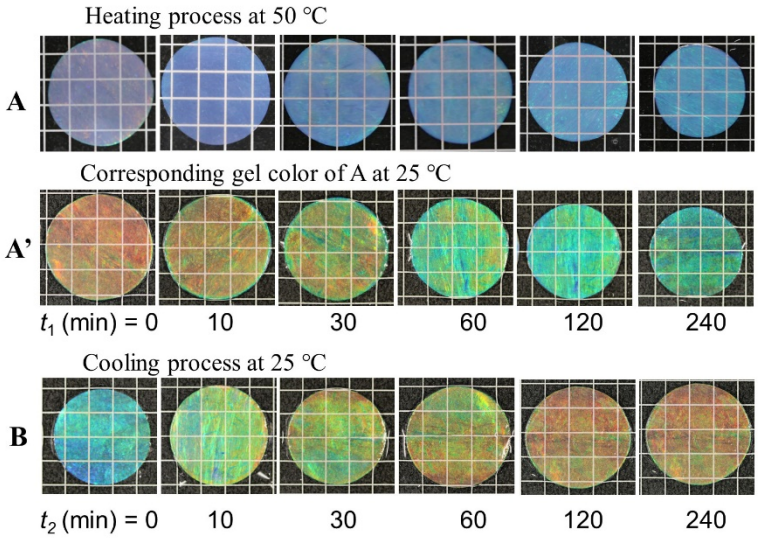

Figure 4-3: Optical images of PDGI/PAAm-PNIPAM$_{0.5M}$ gel during heating and cooling process. The corresponding color of the turbid gel, A', during t_1 was captured immediately after quenching the gel of A in a cold bath (*Temp* = 25 ℃). Background lattices: 5 × 5 mm.

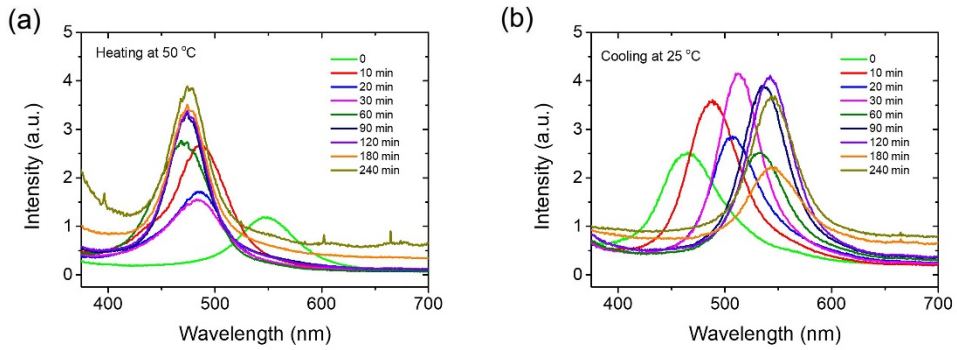

Figure 4-4: (a) Reflection spectra of the PDGI/PAAm-PNIPAM$_{0.5M}$ gel heated at 50 °C for varied t_1 and then quenched in a cold water bath (*Temp* = 25 °C). The spectra were obtained immediately after the quenching. (b) Those of the gel heated at *Temp* = 50 °C for more than 2 h and then cooled in a cold water bath (*Temp* = 25 °C) for varied t_2. The reflection spectra were obtained by keeping the incident at 60^o and reflection angles at 45^o.

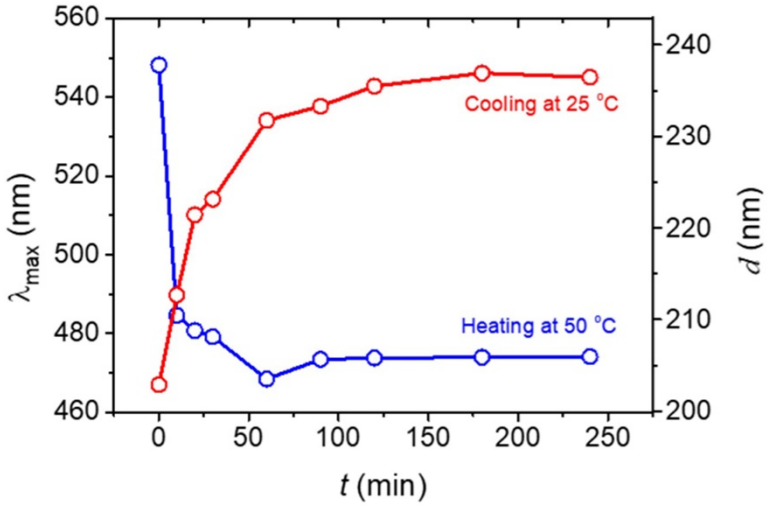

Figure 4-5: Peak wavelength, λ_{max}, of the reflection spectrum and the corresponding interplanar distance, *d*, of PDGI/PAAm-PNIPAM$_{0.5M}$ gel in water as a function of time during heating and cooling process. λ_{max} is measured using Figure 4-3A' samples for the heating process.

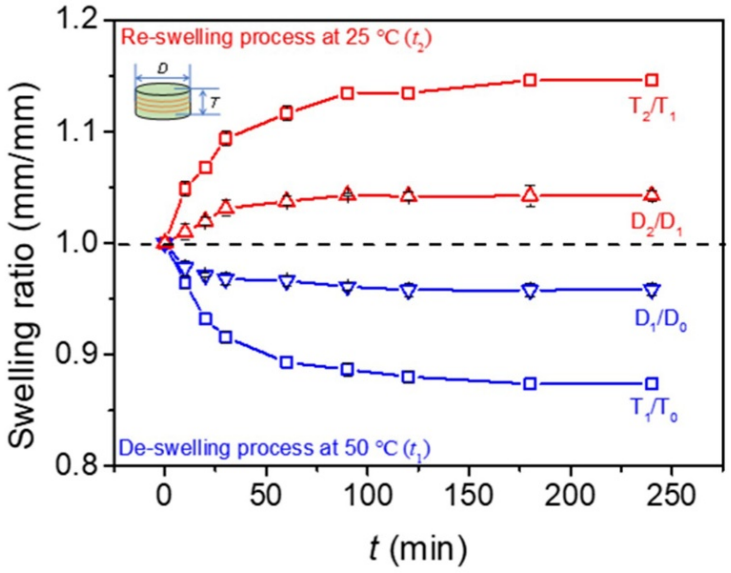

Figure 4-6: Deswelling and reswelling ratios of PDGI/PAAm-PNIPAM$_{0.5M}$ gel in water as a function of time during heating and cooling process.

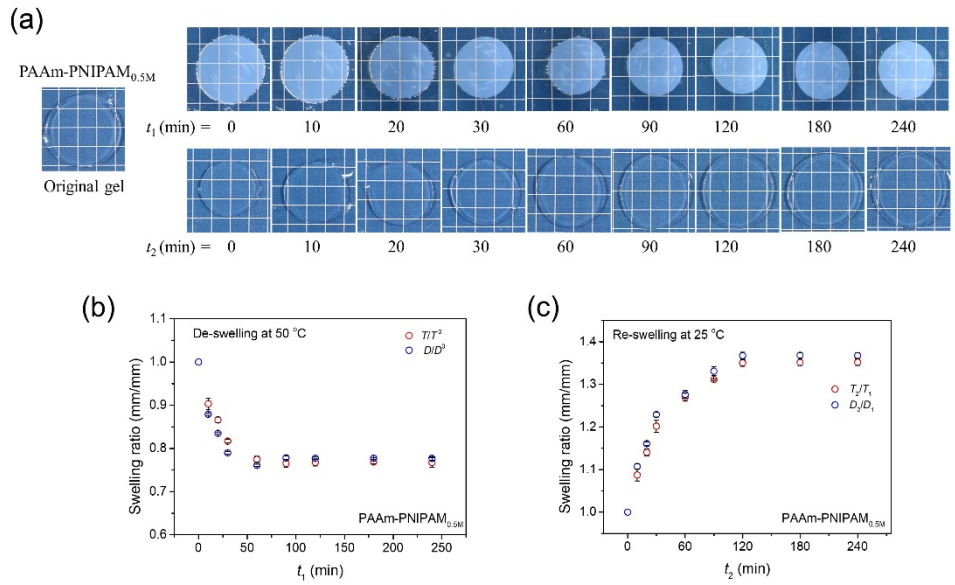

Figure 4-7: Deswelling/reswelling behaviors of the PAAm-PNIPAM$_{0.5M}$ gel during heating and cooling process. (a) Optical images of the original PAAm-PNIPAM$_{0.5M}$ gel at 25 ℃ in pure water that during heating process at 50 ℃ at desired time, t_1 and cooling process at desired time, t_2 at 25 ℃ in pure water; (b) deswelling and reswelling ratios of the PAAm-PNIPAM$_{0.5M}$ gels in water as a function of time during heating and cooling process. Background lattices in (a) are 5 × 5 mm.

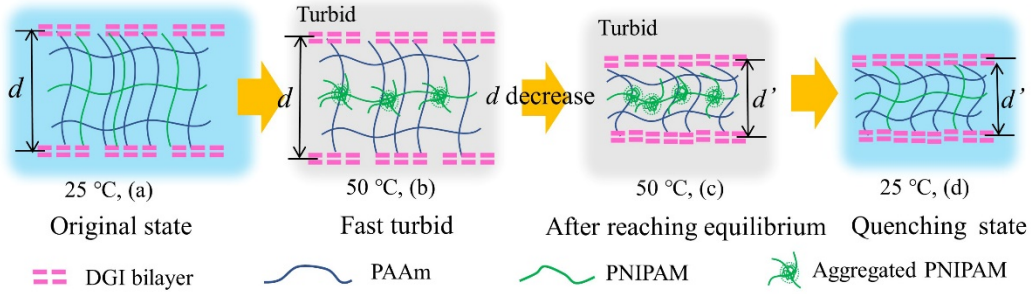

Figure 4-8: Illustration of the thermal-responsively turbid phenomenon of PDGI/PAAm-PNIPAM hydrogel based on lamellar structure during the heating process.

Chapter 5: Effect of PNIPAM concentration

5.1 Introduction

Thermally responsive polymers have been widely applied in many systems, especially in bio-processes, mainly because temperature control is easy to realize and a mild thermal treatment is environmentally benign.[1-3] Among them, Poly(*N*-isopropylacrylamide) (PNIPAM) has been demonstrated to be temperature-responsive polymer and exhibits a lower critical solution temperature (LCST) of 32-33 °C in water.[4] Notably, this critical temperature is often modified by forming copolymers between NIPAM and other monomers.[5] When the temperature is below the LCST, the polymer stays in a swollen hydrated state; above the LCST, it changes to a shrunken dehydrated state.[2] The volume shrinkage of PNIPAM above the LCST induces a sharp lattice and volume contraction. This sequence of events has been extensively employed for preparing thermoresponsive second structures.[6]

The ordered structure of the hydrogels imparts excellent anisotropic functions and makes them promising candidates for applications in sensors, soft robotics, artificial muscles, and biological engineering, owing to their soft and wet nature.[7] Therefore, it is important to develop effective strategies for the fabrication of anisotropic hydrogels possessing highly ordered structures and excellent properties. Among them, novel 2D anisotropic hydrogels having ordered bilayer structures are particularly of interest because of their highly practical properties such as one-dimensional (1D) swelling, anisotropic diffusion, photonic properties manifesting as iridescent structural colors,

and specific mechanical properties (e.g., high fracture strength, anisotropic moduli,self-recovery, and high crack-resistance).[7-11]

Recently, our group has developed a novel 2D anisotropic hydrogels having ordered bilayer structures, PDGI/PAAm.[7-12] The PDGI/PAAm hydrogels prepared using self-assembly and shear force possessed a 1D structure containing thousands of PDGI lamellar bilayers embedded inasoft PAAm hydrogel matrix. Owing to the anisotropic structures composed of highly ordered lamellar bilayers, the PDGI/PAAm hydrogel exhibited remarkable anisotropic swelling and de-swelling behaviors, diffusion, and iridescent structural color. In addition, the gel has stimuli-responsiveness, such as strain-sensitivity (mechanical stimuli), pH/temperature sensitivity (by introduced a secondary network of poly(acrylicacid) (PAAc) into the PAAm layer of a PDGI/PAAm gel to form an inter penetrating soft layer of PAAm-PAAc), ionic-strength sensitivity (by changing a part of the amide groups in the PAAm gellayers into carboxyl groups, generating a polyelectrolyte (sodium polyacrylate) within the gels), electrically responsive/patterning (by developing highly electrically tunable photonic hydrogels based on high-water-content polyelectrolyte polymer networks and bilayer domain structures), and reversible stimuli-responsive patterns (by pressure or pH stumili).[7]

By incorporating secondary functional components into the soft layers of PAAm of PDGI/PAAm hydrogel and under external stumili, the hydrogel could exhibit unique funtionabilities. In this chapter, we introduced a second networks of PNIPAM into the soft layer PAAm of the PDGI/PAAm gels. Hybridization of the thermo-responsive PNIPAM with the PDGI/PAAm hydrogel can give the anisotropic photonic hydrogel

with various fascinating thermo-responsive properties, such as structural color/turbid transition, thermo-responsive structural color, and anisotropic deswelling/reswelling behavior by temperature stimuli. The temperature-induced change in turbidity, structural color and anisotropic swelling of the gel around LCST can be tuned by controlling the incorporated PNIPAM concentration, which can find diverse promising applications, such as smart windows and smart display.

5.2 Experiments

5.2.1 Materials

DGI was synthesized and purified according to our previous work.[8] The DGI fraction was eluted with a hexane/ethyl acetate mixture (1:1 by volume) and was further purified twice by recrystallization from an acetone/hexane mixture (1/1 by weight). *N*,*N*′-methylenebis(acrylamide) (MBAA, 99.0%, FUJIFILM Wako Pure Chemical Corporation, Japan) was recrystallized from ethanol, acrylamide (AAm, 98%, JUNSEI Chemicals Co. Ltd., Japan) was recrystallized from chloroform, *N*-isopropylacrylamide (NIPAM, 97%, Sigma-Aldrich Co., USA) was recrystallized twice from an ether/hexane mixture. 2-Hydroxy-4′-(2-hydroxyethoxy)-2-methylpropiophenone (Irgacure 2959, 98%, Sigma-Aldrich Co., USA) and sodium dodecyl sulfate (SDS, 98%, FUJIFILM Wako Pure Chemical Corporation, Japan) were used as received. Milli-Q deionized water was used to prepare the monomer solutions and for the swelling of the gel.

5.2.2 Transmittance Analysis.

The transmittance of the sample was measured using an ultraviolet/visible light spectrophotometer (UV-1800, SHIMADZU, Japan). The sheet-like gel sample was placed in a quartz cuvette filled with water during measurement. The light was imposed to the top surface of the lamellar gels. The transmittance spectra of the samples in the range of 400-700 nm was measured. The range of 400-700 nm is the wavelength range of visible light. To compare the transmittance in the range of 400-700 nm above and below LCST of PDGI/PAAm-PNIPAM hydrogel samples, a temperature control device was installed and the transmittance at 25 and 50 °C was measured. ITo compare the turbidity of the gel after incorporated PNIPAM networks, the transmittance was measured in the range of 400-700 nm during heating process at 50 °C. The UV light was imposed to the top surface of the lamellar gels. The sample was placed in a quartz cuvette filled with water during measurement. Effect of PNIPAM concentration on the turbidity of PDGI/PAAm-PNIPAM gels at different states were shown in **Figure 5-2**.

5.2.3 Reflection spectrum

The reflection spectrum of various gel samples was measured by a combined setup of light source, variable angle measurement device, and an analyzer. A Xe lamp was used as a light source to obtain the reflection spectrum. Reflection measurement optics with variable angles (Hamamatsu Photonics KK, C10027A10687) were used to detect the reflected light. A photonic multichannel analyzer (Hamamatsu Photonics KK, C10027) was used for analyzing the detected signals. The entire reflection spectrum

was obtained by keeping the incident angle at 60° and reflection angles at 45°. The distance between two lamellar layers, *d*, was roughly calculated using the Bragg's law of diffraction, $\lambda_{max} = 2nd\sin\theta$, where $n = 1.33$ is the refractive index of water, θ is the incident angle, and λ_{max} is the wavelength at maximum reflectance intensity.[12] The reflection spectra of the PDGI/PAAm and PDGI/PAAm-PNIPAM gel with different NIPAM concentration during heating and cooling process around LCST were measured as shown in **Figure 5-4**. The *d* and λ_{max} of the PDGI/PAAm and PDGI/PAAm-PNIPAM gels with different NIPAM concentration at different states during heating and cooling process were compared as shown in **Figure 5-5**.

5.2.4 Swelling Ratio Measurement

For the swelling experiment, a swollen gel was cut into a cylindrical shape using a cylinder cutter (Diameter = 20.00 mm). Diameter of a cylindrical gel at different swollen state, *D*, was measured by a slide caliper. Thickness of the PDGI/PAAm and PDGI/PAAm-PNIPAM gels, *T*, was measured using a mechanical thickness meter (Teclck, Dumb Bell Ltd., Japan).

5.2.5 The drying, UV exposure, and pH tolerance tests

The drying test was conducted during drying in air and recovery in water at 25 °C. The PDGI/PAAm-PNIPAM$_{0.5M}$ gel was exposure to UV for 1 day. The gel during UV exposure was irradiated at 365 nm UV with an intensity of 3.9 mW/cm^2 for 1 day. The pH responsiveness of the PDGI/PAAm-PNIPAM$_{0.5M}$ hydrogel was tested at different pH for 1 day.

5.3 Results and Discussion

5.3.1 Effect of PNIPAM concentration on turbidity

The structural color of PDGI/PAAm-PNIPAM gel can be tuned by controlling PNIPAM concentration. The effect of the NIPAM concentration on the appearance of the PDGI/PAAm-PNIPAM gels at each step. As shown in **Figure 5-1** (a), at room temperature in pure water, the PDGI/PAAm-PNIPAM gel (D ~ 20 mm) exhibits distinctive red-shift in color with increasing incorporated PNIPAM concentration. The color of the PDGI/PAAm-PNIPAM gel changes from green-orange to red and even dark red with an increase in the PNIPAM concentration from 0.25 to 1.0 M. The factor which causes the turbidity of the gel is the phase separation behavior of PNIPAM networks when heating at *Temp* > LCST,[13,14] which is determined by the incorporated PNIPAM concentration. As shown in **Figure 5-1** (b), low concentration gel shows slight turbidity (PDGI/PAAm-PNIPAM$_{0.25M}$), while high concentration gel shows high turbidity (PDGI/PAAm-PNIPAM$_{1.0M}$). After quenching of the gels at this state, the gel color shows large blue shift with increasing NIPAM concentration **Figure 5-1** (c). The gel color shows large blue shift after reaching equilibrium with increasing NIPAM concentration. After reaching recovery equilibrium, all the gels recover to the original color **Figure 5-1** (d).

Effect of the incorporated PNIPAMdensity on the ultrafast turbidity transition was investigated. We facilely tuned the turbidity of PDGI/PAAm-PNIPAM hydrogels with the PNIPAM concentration, *c*. The transmittance of the PDGI/PAAm and

PDGI/PAAm-PNIPAM gels with different *c* at 25 ℃ is shown in **Figure 5-2a**. All the gels exhibit high transmittance. The peaks in the spectra correspond to the structural color. After immersing these gels into 50 ℃ hot water bath, the transmittance of all the PDGI/PAAm-PNIPAM gels decreased immediately, but the samples with higher *c* showed lower transmittance (**Figure 5-2b**). Taken the transmittance at 400 nm as an index, that of the PDGI/PAAm-PNIPAM$_{0.5M}$ gel decreased from 64% to 25%, and that of the PDGI/PAAm-PNIPAM$_{1.0M}$ gel decreased from 69% to 5%. As introduced above, the interpenetration of PNIPAM with PAAm barely affects the phase transition behavior of PNIPAM, but it allows fine-tuning of hydrophobic-hydrophilic balance above LCST. The gels with denser PNIPAM exhibited lower transmittance due to their larger PNIPAM density. Upon this ultrafast transition, the peak wavelength of the spectra, corresponding to the hidden structural color, barely changed.

Basically, samples with higher NIPAM concentrations showed lower transmittance due to their larger PNIPAM density. After 2 h immersion in 50 ℃ hot water, the gel reached new equilibrium at 50 ℃. Upon this long-term deswelling process, the transmittance spectra did not change remarkably but the peak wavelength of the gels exhibited remarkable blue shift, which is in accord with the taken images (**Figure 5-2c** and **Figure 5-1a**).

By quenching the heated shrunken gels into 25 ℃ cold water bath, the gels recovered their high transmittance immediately (**Figure 5-2d and Figure 5-1 (c)**), but the peak wavelength recovered slowly. The peak wavelength of the gels gradually recovered during the long-term reswelling process mainly due to the slow diffusion of

water molecules, which is also in associated with the time-dependent color change during the cooling process.

5.3.2 Effect of PNIPAM concentration on structural color

As shown in **Figure 5-3**, during deswelling process in 50 ℃ hot water bath, the PDGI/PAAm-PNIPAM gels with different NIPAM concentration show clearly blue shift in color with increasing heating time, t_1; during reswelling process in 25 ℃ cold water bath, the PDGI/PAAm-PNIPAM gels with different NIPAM concentration show clearly red shift in color with increasing cooling time, t_2. Particularly, high NIPAM concentration gel shows larger shift in color.

5.3.3 Effect of PNIPAM concentration on interplanar distance

The reflection spectra of PDGI/PAAm, PDGI/PAAm-PNIPAM$_{0.25M}$, and PDGI/PAAm-PNIPAM$_{1.0M}$ gel at different heating time during heating and cooling processes are shown in **Figure 5-4**.

The density of incorporated PNIPAM networks significantly influences the extent of deswelling and reswelling. PDGI/PAAm-PNIPAM hydrogels exhibit a shift in structural color and the peak wavelength shift during heating and cooling process, as revealed by the earlier discussion. To investigate the effect of PNIPAM density on color shift and deswelling/reswelling behavior, the corresponding color and reflection spectra of the PDGI/PAAm-PNIPAM hydrogels with different NIPAM concentrations, *c*, during deswelling and reswelling process were collected. **Figure 5-5** shows the change in λ_{max} and d for the PDGI/PAAm-PNIPAM hydrogels with different c during

deswelling and reswelling as a function of t_1 and t_2. The higher c was, the greater the extent of the decrease/increase in λ_{max} and d during the heating/cooling process became. This indicates that the PNIPAM density plays a rule in the variations of λ_{max} and d, which is in accord with the color shift of the gel. It is worth mentioning that the time to reach equilibrium is almost independent of c because the timescale is dominated by the water diffusion.

5.3.4 Effect of PNIPAM concentration on anisotropy deswelling/reswelling

The effect of the incorporated PNIPAM density on anisotropy deswelling/reswelling is shown in **Figure 5-6**. The extent of deswelling/reswelling increased with c. On the other hand, swelling anisotropy became less obvious with increasing c. PNIPAM is incorporated into the PAAm layer of PDGI/PAAm hydrogels, forming an interpenetrating soft layer of PAAm-PNIPAM within the hydrogels. Such incorporation of the PNIPAM network adds additional osmotic pressure to the gel. At low c (0.25 M), incorporating the PNIPAM networks into PAAm layers leads to negligible swelling of the gels, as a result, the bilayer structure remains intact. Therefore, the gels show negligible in-plain deswelling/reswelling ($D_1/D_0 \sim 1.00$). With increasing c, the addition of PNIPAM networks induces remarkable swelling of the gel layers, which gives tension and damage to the PDGI bilayers. Because of the partial fracture of the PDGI bilayers, the anisotropy in deswelling/reswelling of the PDGI/PAAm-PNIPAM hydrogels weakens as observed from the slight deswelling along the diameter direction ($D_1/D_0 \sim 0.96$ for 0.5 M, $D_1/D_0 \sim 0.93$ for 1.0 M). In addition, the structural

color of the gels became less obvious with increasing *c*, which may be attributed to a weaker reflection of light at the bilayer-network interfaces. The reason for the weaker reflection is not clear but might be related to the change in the refractive index of the gel layers after the incorporation of PNIPAM.

5.3.5 Effect of PNIPAM concentration on reversibility

To investigate the effect of PNIPAM density on the swelling reversibility of the gel during the heating and cooling process, the photographs and reflection spectra of PDGI/PAAm and PDGI/PAAm-PNIPAM with different *c* after reaching deswelling and reswelling equilibrium are shown in **Figure 5-7**. The appearance of the gels at the original state and the deswelling equilibrium state are shown in **Figure 5-7a** and **5-7b**, respectively. The original hydrogels show a red shift in gel color with increasing NIPAM concentration (**Figure 5-7a**). After reaching deswelling equilibrated state, high NIPAM concentration gel exhibits clearly distinct blue shift in gel color (**Figure 5-7b**). After reswelling process, the hydrogels almost fully recovered to the original color (**Figure 5-7c**). The reflection spectra of the hydrogels at the original state and deswelling equilibrium states are shown in **Figure 5-7d**. After deswelling process, the hydrogels show a bule shift in peak wavelength (**Figure 5-7e**). The peak wavelength recovered almost completely after reswelling (**Figure 5-7f**). The corresponding λ_{max} and *d* of the original gels were shown in **Figure 5-7g**. Along with the blue shift in color, λ_{max} and *d* apparently decreased for different NIPAM concentration gels (**Figure 5-7h**) and then recovered after fully reswelling (**Figure 5-7i**). The corresponding λ_{max} and *d*

of the gels also exhibited the same trends. These results indicate that fully reversible color shift of the PDGI/PAAm-PNIPAM gels upon heating-cooling cycles is independent of the PNIPAM density. Consequently, changing the PNIPAM density has a negligible effect on the swelling reversibility of the PDGI/PAAm-PNIPAM gels.

The repeatability the structural color change of the PDGI/PAAm-PNIPAM hydrogel upon multiple heating-cooling cycles around LCST was further demonstrated (**Figure 5-8**). The PDGI/PAAm-PNIPAM$_{0.5M}$ gel recovered to the original color after each heating and cooling process (**Figure 5-8a**). The reflection spectra of PDGI/PAAm-PNIPAM$_{0.5M}$ gel after each heating and cooling process around LCST was shown in **Figure 5-8b**. The λ_{max} and d after each heating and cooling processes remained very small (within ±10 nm) as shown in **Figure 5-8c**. It indicates that the gel shows high reversibility in gel color and lamellar distance after each process. The full width at half maximum (FWHM) of the reflection spectra of the gel as a function of number of recovery times also showed negligible fluctuation, which indicates that the properties of the gel barely changed and the gel possesses excellent stability and reversibility. Remarkably, the gel maintained its high turbidity during a one-month immersion in a hot water bath (**Figure 5-9**). The original PDGI/PAAm-PNIPAM$_{0.5M}$ gel, which was initially red at 25 ℃ cold water bath, turned turbid when heated at 50 ℃ hot water bath. Remarkably, it maintained its turbidity during a one-month immersion in the hot water bath. Once quenching the gel in a 25 ℃ cold water bath, the turbidity disappeared, and the gel turned blue. After cooling for 4 hours in a 25 ℃ cold water bath, the blue gel gradually regained its original red color.

In addition, the gel size (thickness and diameter) upon the multiple cycles also has been investigated to prove the high reversibility (**Figure 5-10**). The cycle number has no effect on the anisotropic deswelling/reswelling (**Figure 5-10a**), suggesting that the PDGI/PAAm-PNIPAM$_{0.5M}$ gel exhibits the highly reversible in anisotropic swelling behavior (**Figure 5-10b**).

The thickness and diameter after each heating and cooling process of the PDGI/PAAm-PNIPAM$_{0.5M}$ gel are measured and shown in **Figure 5-10**. Except for the first heating process, the thickness and diameter of the gel after each heating process were at the same minimum value, indicating that the number of the heating processes does not affect deswelling (**Figure 5-10a**). The diameter and thickness of the gel almost recovered their original value after each cooling process (**Figure 5-10b**). It indicated that PDGI/PAAm-PNIPAM gel exhibits highly thermo-reversible properties.

As shown in **Figure 5-11a**, during the drying process in air, the gel gradually released water, resulting in a noticeable blue shift in its color. After 6 h drying, the gel transformed into a transparent state. Immersing the dried gel back to water at 25 °C, the gel gradually absorbed water and recovered its original color. The gel shows no responsiveness to UV exposure (**Figure 5-11b**) or pH (**Figure 5-11c**).

5.4 Conclusion

We have successfully synthesized a thermally responsive photonic hydrogel with lamellar structure, not only exhibiting reversibly anisotropic deswelling/reswelling properties due to phase separation behavior near LCST, but also permitting structural

color, turbidity, and anisotropic swelling by controlling incorporated LCST-type networks.

In this chapter, we prepared PDGI/PAAm and PDGI/PAAm-PNIPAM hydrogels with different concentration and investigated the effect of PNIPAM concentration on the hydrogels, including the turbidity, structural color shift (switching of the stop-band), the interplanar distance, anisotropy deswelling/reswelling, and reversibility during heating and cooling process around LCST. In conclusion, the PDGI/PAAm-PNIPAM hydrogel shows ultrafast turbidity transition during heating and cooling process around LCST, and the extent of turbidity is determined by the NIPAM concentration. Besides, the gel exhibits color tunable characteristics, which is controlled by the concentration of interpenetrating second PNIPAM networks into the first PAAm soft layers. The hydrogel turns blue-shift in color during heating at *Temp* > LCST and turns red-shift as well as recovers to the original color during cooling *Temp* < LCST. In addition, the extent of deswelling/reswelling increases with the NIPAM concentration. On the other hand, swelling anisotropy became less obvious with the NIPAM concentration. The gels recovered to the original state upon cooling process, indicating fully reversible color shift independent of the NIPAM concentration.

The drying, UV exposure, and pH tolerance tests for the hybrid hydrogels were also conducted to evaluate the stability, repeatability, and durability of the PDGI/PAAm-PNIPAM hydrogel against harsh conditions. The gel exhibited remarkable stability against the drying and reswelling treatment, and it was unresponsive to both UV exposure and pH change.

Reference

[1] Z. Li, Q. Fan, Y. Yin. Colloidal Self-Assembly Approaches to Smart Nanostructured Materials. *Chem. Rev.* **2022**, 122, 4976-5067.

[2] G. Ju, M. Cheng, M. Xiao, J. Xu, K. Pan, X. Wang, Y. Zhang, F. Shi. Smart Transportation Between Three Phases Through a Stimulus-Responsive Functionally Cooperating Device. *Adv. Mater.* **2013**, 25, 2915-2919.

[3] Y. J. Kim, Y. T. Matsunaga. Thermo-responsive Polymers and Their Application as Smart Biomaterials. *J. Mater. Chem. B* **2017**, 5, 4307-4321.

[4] C. De las Heras Alarcón, S. Pennadam, C. Alexander. Stimuli Responsive Polymers for Biomedical Applications. *Chem. Soc. Rev.* **2005**, 34, 276-285.

[5] S. Lanzalaco, E. Armelin. Poly (*N*-isopropylacrylamide) and Copolymers: A Review on Recent Progresses in Biomedical Applications. *Gels* **2017**, 3, 36.

[6] L. Tang, L. Wang, Y. Xiao, Y. Feng, Y. Li, W. Feng. Poly(*N*-isopropylacrylamide)-Based Smart Hydrogels: Design, Properties and Applications. *Prog. Mater. Sci.* **2021**, 115, 100702.

[7] Y. Yue, J. P. Gong. Structure and Unique Functions of Anisotropic Hydrogels Comprising Uniaxially Aligned Lamellar Bilayers. *Bull. Chem. Soc. Jpn.* **2021**, 94, 2221-2234.

[8] M. A. Haque, G. Kamita, T. Kurokawa, K. Tsujii, J. P. Gong. Unidirectional Alignment of Lamellar Bilayer in Hydrogel: One-Dimensional Swelling, Anisotropic Modulus, and Stress/Strain Tunable Structural Color. *Adv. Mater.* **2010**, 22, 5110-5114.

[9] M. A. Haque, T. Kurokawa, G. Kamita, Y. Yue, J. P. Gong. Rapid and Reversible Tuning of Structural Color of a Hydrogel over the Entire Visible Spectrum by Mechanical Stimulation. *Chem. Mater.* **2011**, 23, 5200-5207.

[10] Y. F. Yue, M. A. Haque, T. Kurokawa, T. Nakajima, J. P. Gong. Lamellar Hydrogels with High Toughness and Ternary Tunable Photonic Stop-Band. *Adv. Mater.* **2013**, 25, 3106-3110.

[11] M. A. Haque, T. Kurokawa, T. Nakajima, G. Kamita, Z. Fatema, J. P. Gong. Surfactant Induced Bilayer-Micelle Transition for Emergence of Functions in Anisotropic Hydrogel. *J. Mater. Chem. B* **2022**, 10, 8386-8397.

[12] K. Mito, M. A. Haque, T. Nakajima, M. Uchiumi, T. Kurokawa, T. Nonoyama, J. P. Gong. Supramolecular Hydrogels with Multi-Cylindrical Lamellar Bilayers: Swelling-Induced Contraction and Anisotropic Molecular Diffusion. *Polymer* **2017**, 128, 373-378.

[13] Y. Ding, X. Zhang, B. Xua, W. Li. LCST and UCST-type Thermoresponsive Behavior in Dendronized Gelatins. Polym. Chem., 2022, 13, 2813-2821.

[14] C. Yu, K. Cui, H. Guo, Y. N. Ye, X. Li, J. P. Gong. Structure Frustration Enables Thermal History-Dependent Responsive Behavior in Self-Healing Hydrogels. Macromolecules 2021, 54, 9927-9936.

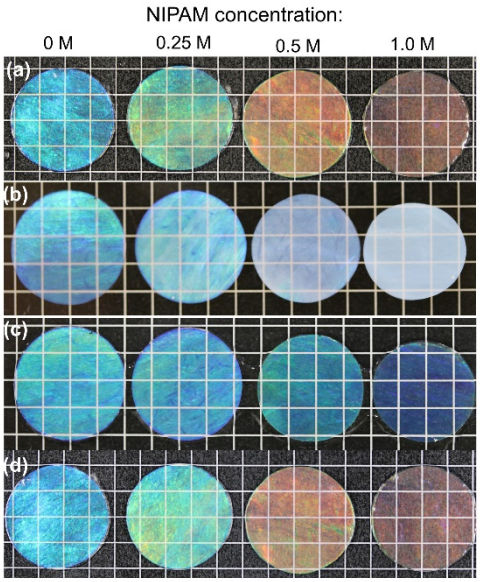

Figure 5-1: Optical images of the PDGI/PAAm, PDGI/PAAm-PNIPAM$_{0.25M}$, PDGI/PAAm-PNIPAM$_{0.5M}$ and PDGI/PAAm-PNIPAM$_{1.0M}$ gels at different state during the heating process at 50 ℃ and cooling process at 25 ℃ in pure water: (a) original state 25 ℃, (b) after reaching new equilibrated state at 50 ℃, (c) quenched state at 25 ℃ after reaching de-swollen equilibrium, and (d) recovery state at 25 ℃. The corresponding color of the turbid gel after reaching a new equilibrium during the heating process was captured immediately after quenching the gel in a cold water bath (*Temp* = 25 ℃). Background lattices are 5 × 5 mm.

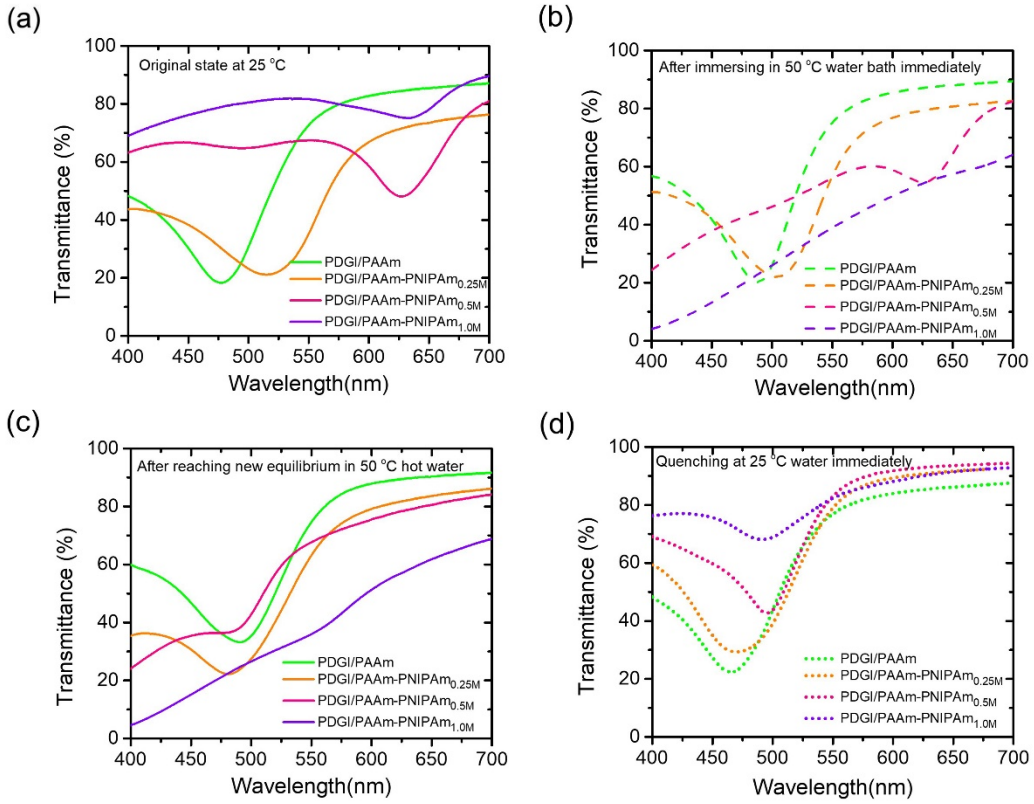

Figure 5-2: Effect of NIPAM concentration on the turbidity of the PDGI/PAAm-PNIPAM gels. Transmittance of the PDGI/PAAm and PDGI/PAAm-PNIPAM gels with different NIPAM concentrations at (a) original state, (b) after immersing in 50 ℃ water bath immediately, (c) after reaching new equilibrium into 50 ℃ water bath, and (d) quenching state at 25 ℃ water bath after reaching new equilibrium into 50 ℃ water bath. The transmittance was measured immediately after the samples were transferred to the hot or cold bath.

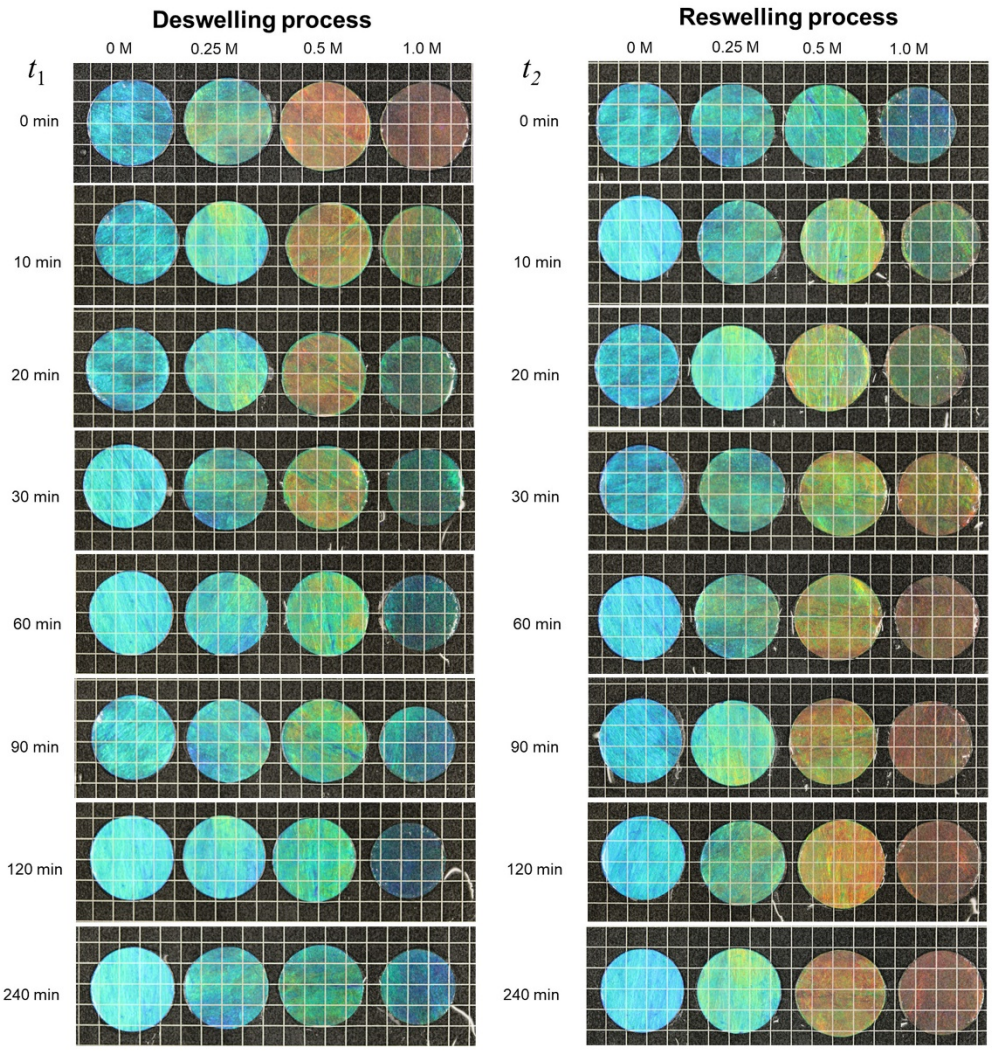

Figure 5-3: Optical images of the PDGI/PAAm, PDGI/PAAm-PNIPAM$_{0.25M}$, PDGI/PAAm-PNIPAM$_{0.5M,}$ and PDGI/PAAm-PNIPAM$_{1.0M}$ gels during the deswelling process at 50 ℃ for t_1 and reswelling process at 25 ℃ for t_2. The corresponding color of the gel during the deswelling process was captured immediately after quenching the gel in a cold water bath (*Temp* = 25 ℃). Background lattices: 5 × 5 mm.

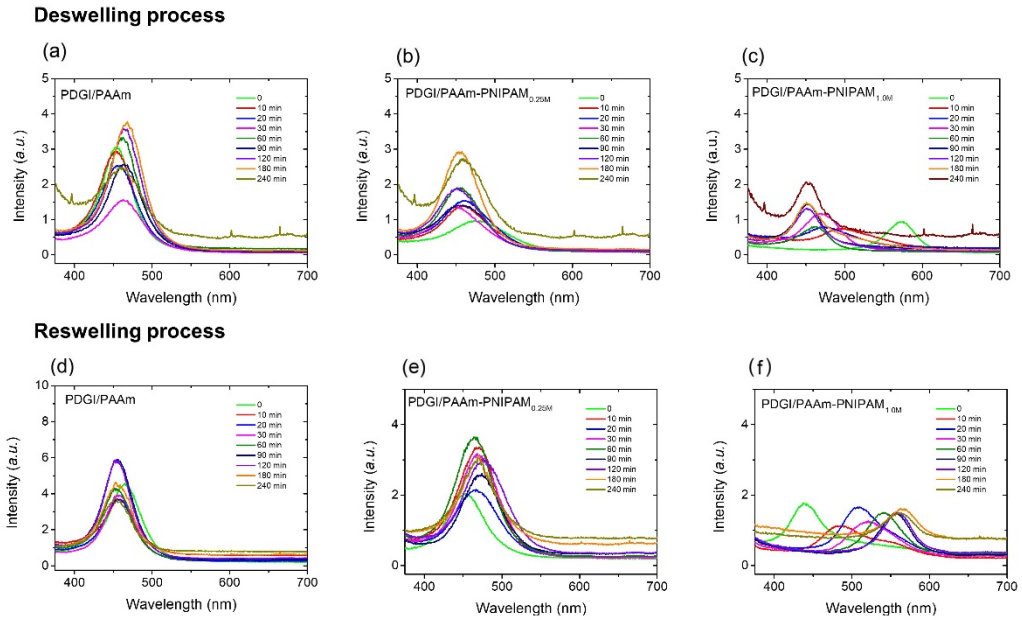

Figure 5-4: Reflection spectra of (a,d) PDGI/PAAm, (b,e) PDGI/PAAm-PNIPAM$_{0.25M}$, and (c,f) PDGI/PAAm-PNIPAM$_{1.0M}$ gel in water during the heating process at 50℃ (a-c) and cooling process at 25℃ (d-f). The corresponding reflection spectra of the gel at different heating time was captured after quenching the gel in a cold bath (*Temp* = 25 ℃). The reflection spectra were obtained by keeping the incident at 60^{o} and reflection angles at 45^{o}.

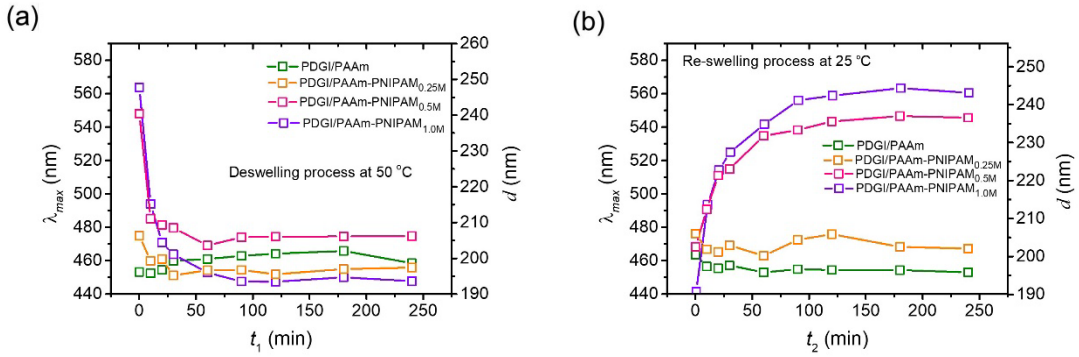

Figure 5-5: Deswelling and reswelling behaviors of PDGI/PAAm and PDGI/PAAm-PNIPAM gels with different NIPAM concentration during heating and cooling process. λ_{max} of the reflection spectrum and *d* as a function of (a) heating (t_1) and (b) cooling time (t_2).

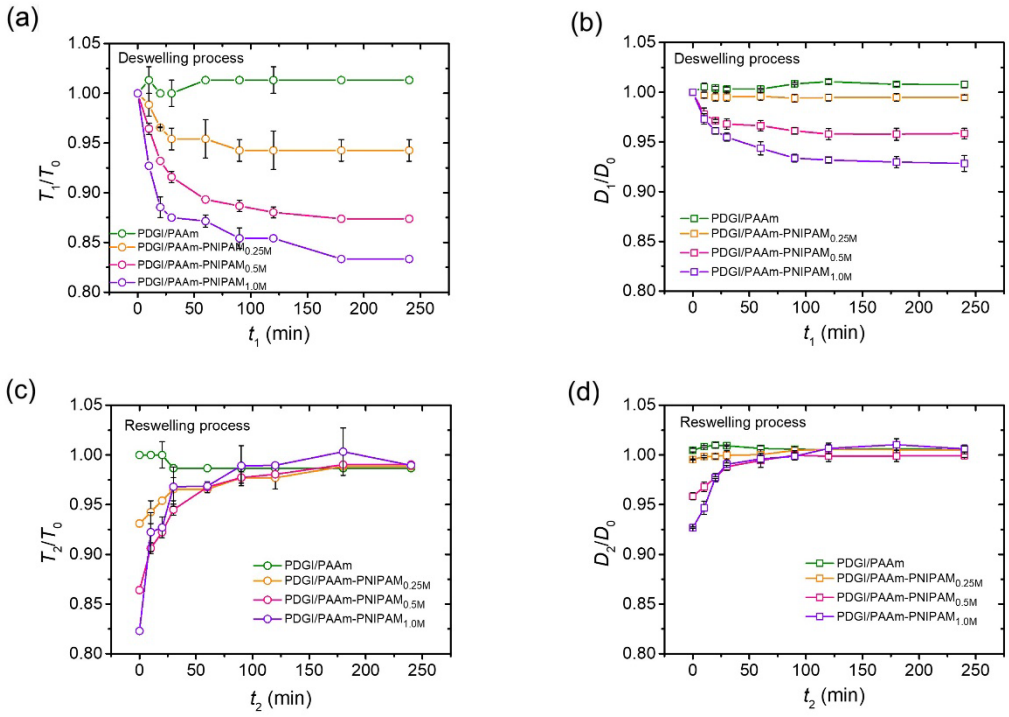

Figure 5-6: Deswelling and reswelling behaviors of PDGI/PAAm and PDGI/PAAm-PNIPAM gels with different NIPAM concentration during heating and cooling process. (a,b) deswelling ratios in water as a function of heating time along the thickness : T_1/T_0 (a) and the diameter: D_1/D_0 (b) direction; (c,d) reswelling ratios in water as a function of cooling time along the thickness: T_2/T_0 (c) and the diameter: D_2/D_0 (d) direction compared to original state.

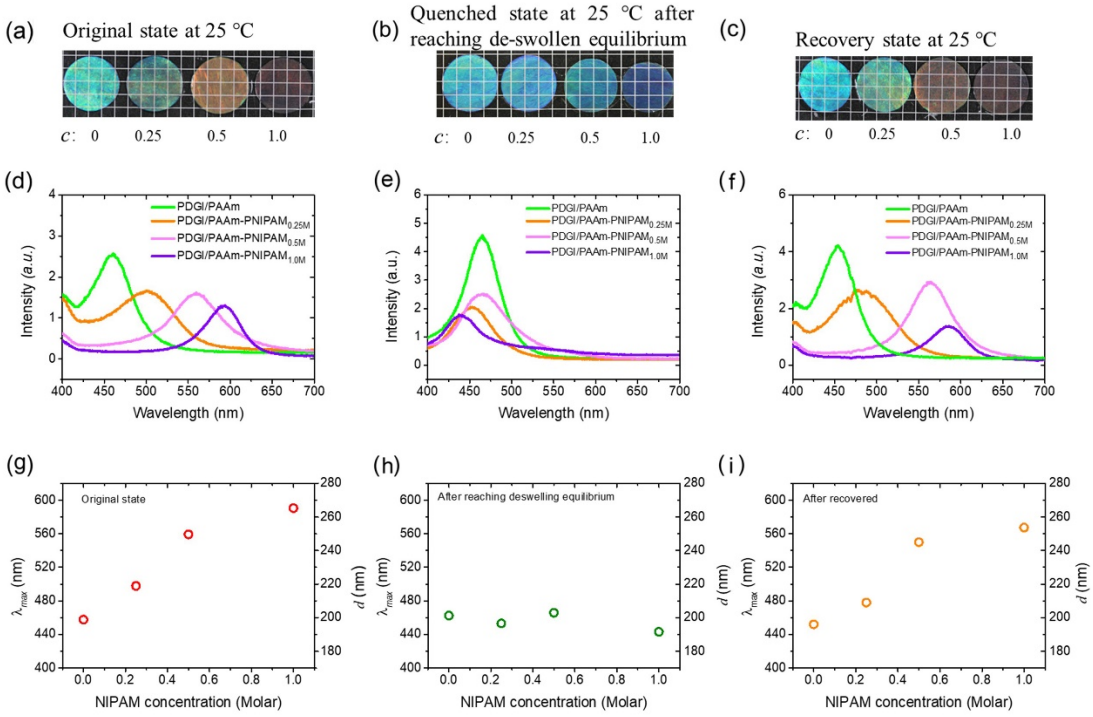

Figure 5-7: Reversibility in the structural color of the PDGI/PAAm and PDGI/PAAm-PNIPAM gels with different NIPAM concentrations, *c*, during the heating and cooling process. (a-c) Photographs, (d-f) reflection spectra, and (g-i) λ_{max} and *d* as a function of the NIPAM concentration of PDGI/PAAm and PDGI/PAAm-PNIPAM gels with different NIPAM concentration at original state (a, d, g), deswelling equilibrium state (b, e, h), and recovery state (c, f, i).

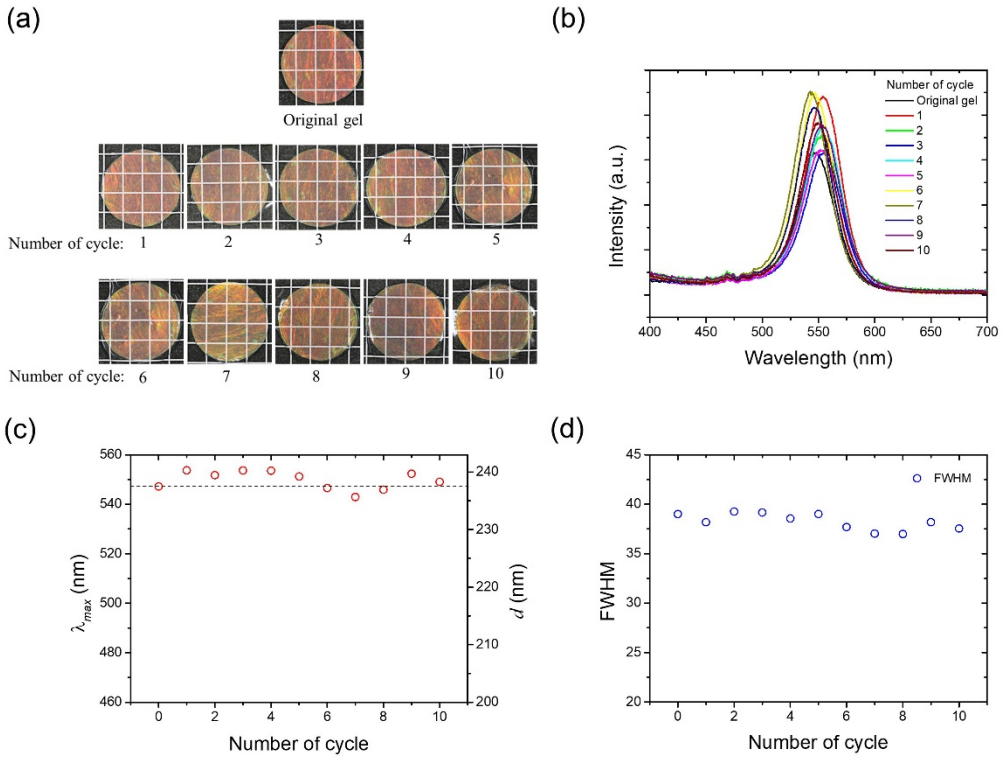

Figure 5-8: (a) Photographs and (b) reflection spectra of the PDGI/PAAm-PNIPAM$_{0.5M}$ gel after experiencing several heating-cooling cycles. The heating-cooling cycle consists of heating at 50 ℃ hot water bath for 4 h and cooling at 25 ℃ cold water bath for 4 h. (c) Peak wavelength, λ_{max}, of the reflection spectrum and the corresponding interplanar distance, *d*, as a function of number of cycles; (d) The full width at half maximum (FWHM) of the reflection spectra of the gel as a function of number of cycles. Background lattices in (a): 5 × 5 mm.

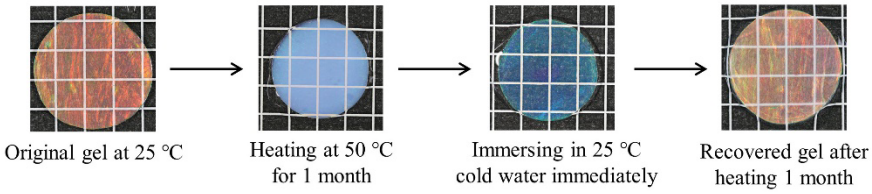

Figure 5-9: Photographs of the PDGI/PAAm-PNIPAM$_{0.5M}$ gel after heating in 50 ℃ hot water bath for 1 month. Background lattices: 5 × 5 mm.

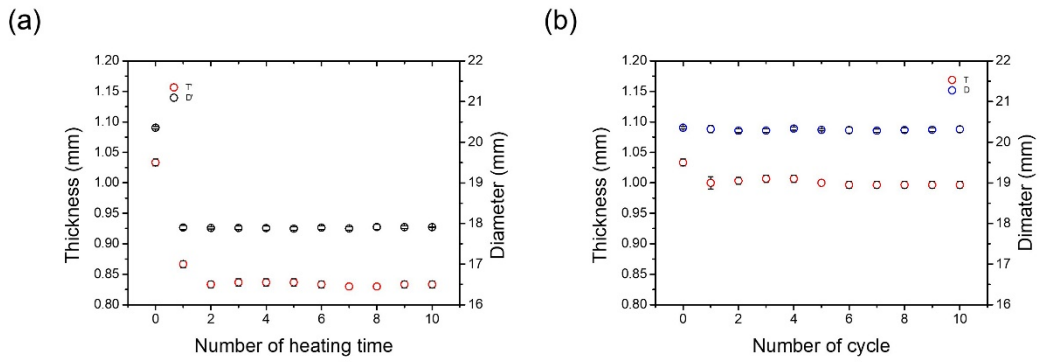

Figure 5-10: (a) Thickness (left axis) and diameter (right axis) of the PDGI/PAAm-PNIPAM$_{0.5M}$ gel in water after heating at 50 ℃ hot water bath for 4 h as a function of heating times (after each heating process, the gel was put back to 25 ℃ cold water bath for 4 h to recover); and (b) thickness (left axis) and diameter (right axis) of PDGI/PAAm-PNIPAM$_{0.5M}$ gel in 25 ℃ water during heating at 50 ℃ hot water bath for 4 h and cooling at 25 ℃ cold water bath for 4 h as a function of the number of heating-cooling cycles.

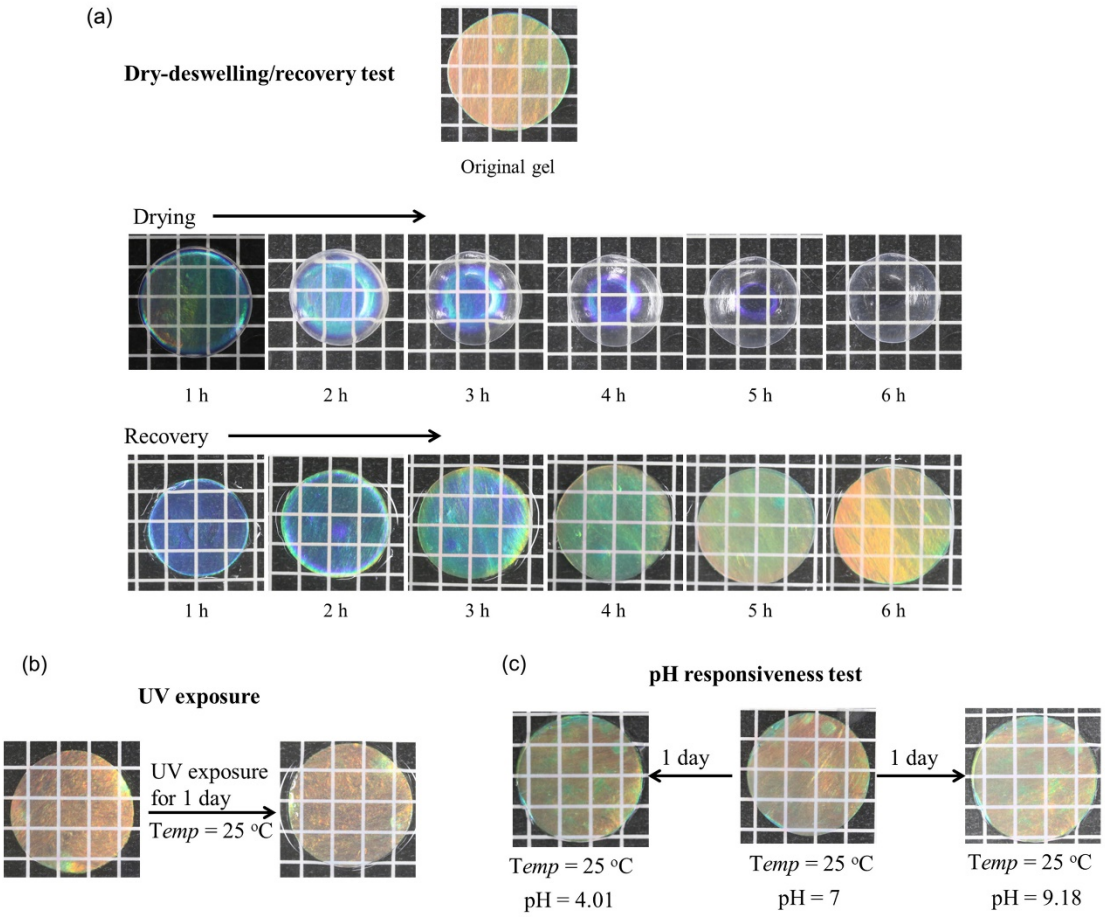

Figure 5-11: The structural color of the PDGI/PAAm-PNIPAM$_{0.5M}$ gel (a) during drying in air and recovery in water at 25 °C, (b) during UV exposure for 1 day, (c) at different pH for 1 day. The gel during UV exposure was irradiated at 365 nm UV with an intensity of 3.9 mW/cm^2 for 1 day.

Chapter 6: Regioselective thermo-responsiveness

6.1 Introduction

Stimuli-responsive colors are a unique characteristic of certain animals, evolved as either a method to hide from enemies and prey or to communicate their presence to rivals or mates.[1,2] From a material science perspective, the solutions developed by Mother Nature to achieve these effects are a source of inspiration to scientists for decades. Photonic crystals, on the other hand, are 2D or 3D periodic structures with low- and high-refractive-index parts, leading to only selective wavelengths to be reflected by the crystal.[3-6] Many animals and plants use a combination of different structural colorations' mechanisms, sometimes also including pigmentary coloration, to achieve the desired colors combination. The use of biomimicry to try and replicate the structural colors of living systems is quite challenging, because much still has to be learned from the perfection and the complexity of the architectures used by Mother Nature. Stimuli-responsive structural colors have an obviously more complex architecture.[1,2] They require the ability to change the microstructure in response to a stimulus. Stimuli-responsive structural colors could have potential applications for the creation of smart sensors, of cloaking devices, of intelligent textiles.[7]

Nowadays, extensive research interest in PNIPAM-based smart hydrogels has been aroused owing to their fascinating properties and functions.[8-10] For example, both the volume phase transition temperature and the extent of the swelling/shrinking process of PNIPAM-based smart hydrogels can be easily controlled through

copolymerization with more hydrophilic or more hydrophobic monomers. It is worth mentioning that the property changes of PNIPAM-based smart hydrogels can be triggered in various ways, including through direct heating, indirect heating (e.g., based on photothermal effect[11,12], Joule heating[13] and hysteresis effect[14]), photoionization[15], or photoisomerization[16], thus allowing sensitivity to temperature, light, electrical field, and magnetic field. Importantly, the unprecedented properties of PNIPAM-based smart hydrogels permit various smart functions, such as shape change, self-regulation and rupture, similar to a cell and some smart biological systems. For example, the change in volume allows the PNIPAM-based smart hydrogels to self-regulate or gate a system by governing the material transportation (i.e., blocking the channels by swelling or opening the channels by shrinking), which is of critical importance in the areas of smart valves[17], water purification[18], drug delivery[19], etc. After being integrated into internal anisotropic hydrogels, the size change of PNIPAM-based smart hydrogels can realise shape change functions like Venus flytrap[20]. When the PNIPAM-based smart hydrogels are fabricated into periodic structures, such as colloidal crystals, the size change can enable the tunable vivid colouration reproducing the iridescence or structural colors in the nature, which find numerous applications for the development of smart optical sensors, intelligent textiles, cloaking and camouflage devices, just to mention a few[2]. The temperature-induced transparency change has shown great potential in smart windows with the functions of self-regulation in solar energy and transmission.[21]

6.2 Experiments

6.2.1 Materials

DGI was synthesized and purified according to our previous work.[22,23] The DGI fraction was eluted with a hexane/ethyl acetate mixture (1:1 by volume) and was further purified twice by recrystallization from an acetone/hexane mixture (1/1 by weight). *N*,*N*′-methylenebis(acrylamide) (MBAA, 99.0%, FUJIFILM Wako Pure Chemical Corporation, Japan) was recrystallized from ethanol, acrylamide (AAm, 98%, JUNSEI Chemicals Co. Ltd., Japan) was recrystallized from chloroform, *N*-isopropylacrylamide (NIPAM, 97%, Sigma-Aldrich Co., USA) was recrystallized twice from an ether/hexane mixture. 2-Hydroxy-4′-(2-hydroxyethoxy)-2-methylpropiophenone (Irgacure 2959, 98%, Sigma-Aldrich Co., USA) and sodium dodecyl sulfate (SDS, 98%, FUJIFILM Wako Pure Chemical Corporation, Japan) were used as received. Milli-Q deionized water was used to prepare the monomer solutions and for the swelling of the gel.

6.2.2 Preparation of photomask

A black lighttight photomask with a hollow star was cut using a laser cutter machine (ULTRA R5000, Universal Laser Systems, Inc.). The PDGI/PAAm lamellar hydrogels immersed in the NIPAM solution is covered by a photomask with a hollow star before synthesis.

6.2.3 Regioselective synthesis

The PDGI/PAAm lamellar hydrogels immersed in the NIPAM solution for 7 days to reach equilibrium. The star PDGI/PAAm-PNIPAM hydrogel in PDGI/PAAm hydrogel was UV-irradiated through photomasking at 4 ℃ for 8 h. Only the UV-irradiated star area turned red after reaching equilibrium in pure water at *Temp* = 25 ℃.

6.3 Results and Discussion

6.3.1 Regioselective synthesis of thermo-responsive lamellar hydrogel

The unique ultrafast structural color/turbid (white) transition of the PDGI/PAAm-PNIPAM hydrogels can be potentially applied as smart windows and smart displays that respond to external environments.[8] Toward such applications, we regioselectively introduced the PNIPAM networks into the PDGI/PAAm lamellar hydrogels by the photomasking during UV polymerization. As shown in **Figure 6-1**, the PDGI/PAAm lamellar hydrogels immersed in the NIPAM solution is covered by a photomask with a hollow star and UV-irradiated at 4 ℃ for 8 h. Only the UV-irradiated star area turned red after reaching equilibrium in pure water at *Temp* = 25 ℃, which indicates that the NIPAM networks can only incorporate into the specific region by controlling UV polymerization area.

6.3.2 Structural color/turbid transition of PDGI/PAAm-PNIPAM gel pattern

As shown in **Figure 6-2**, the original PDGI/PAAm-PNIPAM gel pattern in PDGI/PAAm gel is red color in pure water *Temp* = 25 ℃. To investigate the structural

color/white transition of the pattern, the original gel was immersed in 50 ℃ hot water for 4 h. The original patterned gel shows short-term turbid phenomenon once immersed in 50 ℃ hot water and the turbidity didn't decay during heating (**Figure 6-2, up**). By quenching the gel into cold water, the turbidity disappears immediately and the bright structural color of the pattern appears again (**Figure 6-2, middle**). When the heated pattern gel is quenched in 25 ℃ cold water for long time, the turbidity of the pattern disappears immediately once immersing in cold water (short-term) and dark-blue star gradually absorbs water and recovers to the original red color (long-term, **Figure 6-2, below**).

The structural color/turbid transition of the PDGI/PAAm-PNIPAM gel pattern in PDGI/PAAm is shown in **Figure 6-3**. Upon immersion of the gel into hot water at 50 ℃, the star region immediately got turbid owing to the thermo-induced phase separation of PNIPAM. Like the normal PDGI/PAAm-PNIPAM hydrogels, the star region in the gel exhibited long-term shrinkage with blue-shift in gel color upon heating and recovery of the structural color upon cooling. With increasing heating time, long-term blue-shift in gel color due to the decrease in the layer distance in responsive of the heating-induced shrinking of the PNIPAM networks. This immediate structural color/turbid transition and long-term structural color shift of patterned gel can be used as smart stained glass or smart display.

Patterned gel with immediate structural color/turbid transition and long-term structural color shift has interesting potential applications, particularly as a smart window material or a smart display. This immediate structural color/turbid transition

and long-term structural color shift of patterned gel can be used as smart stained glass or smart display. For example, considering its application as a smart window material, this pattern gel has a mosaic-like structural color similar with stained glass at low temperature. On the other hand, when exposed to strong sunlight, the pattern becomes cloudy due to the temperature increase, providing a smart function to prevent rising of the room temperature.

6.4 Conclusion

In conclusion, patterned gel with immediate structural color/turbid transition holds great promise as a versatile material with applications in various fields, most notably as smart windows and decorative elements. Its ability to dynamically change appearance and control heat transmission makes it an attractive option for enhancing energy efficiency and aesthetic appeal in buildings.

This work has achieved an anisotropic thermo-responsive photonic hydrogel with extensive and reversible structural color tunability based on the lamellar structure. This tunability is rooted in the lamellar structure and is controlled by temperature and the density of PNIPAM. More importantly, the thermo-responsive components can be regioselectively incorporated into the base lamellar gel. This work has demonstrated an astonishingly rapid response in the structural color/turbid transition of this patterned lamellar gel, occurring within a mere 1-second timespan. The structural color/turbid transition observed in this work represents a unique approach in smart window technology. Unlike traditional smart window materials that rely on a transparent-to-

turbid transition triggered by temperature changes, this work achieves a structural color/turbid transition. This distinctive feature sets it apart and offers new possibilities and advantages for smart window applications.

Reference

[1] Y. Ohtsuka, M. Sakai, T. Seki, R. Ohnuki, S. Yoshioka, Y. Takeoka. Stimuli-Responsive Structural Colored Gel That Exhibits the Three Primary Colors of Light by Using Multiple Photonic Band Gaps Acquired from Photonic Balls. *ACS Appl. Mater. Interfaces* **2020**, 12, 54127-54137.

[2] G. Isapour, M. Lattuada. Bioinspired Stimuli-Responsive Color-Changing Systems. *Adv. Mater.* **2018**, 30, 1707069.

[3] M. C. Chiappelli, R. C. Hayward. Photonic Multilayer Sensors from Photo-Crosslinkable Polymer Films. *Adv. Mater.* **2012**, 24, 6100-6104.

[4] A. K. Yetisen, H. Butt, L. R. Volpatti, I. Pavlichenko, M. Humar, S. J. Kwok, H. Koo, K. S. Kim, I. Naydenova, A. Khademhosseini, S. K. Hahn, S. H. Yun. Photonic Hydrogel Sensors. *Biotechnol. Adv.* **2016**, 34, 250-271.

[5] J. Chen, L. Xu, M. Yang, X. Chen, X. Chen, W. Hong. Highly Stretchable Photonic Crystal Hydrogels for a Sensitive Mechanochromic Sensor and Direct Ink Writing. *Chem. Mater.* **2019**, 31, 8918-8926.

[6] I. B. Burgess, L. Mishchenko, B. D. Hatton, M. Kolle, M. Loncar, J. Aizenberg. Encoding Complex Wettability Patterns in Chemically Functionalized 3D Photonic Crystals. *J. Am. Chem. Soc.* **2011**, 133, 12430-12432.

[7] Y. Arai, N. Yashiro, Y. Imura, K. H. Wang, T. Kawai. Thermally Tunable Structural Coloration of Water/Surfactant/Oil Emulsions. *Langmuir* **2022**, 38, 569-575.

[8] L. Tang, L. Wang, X. Yang, Y. Feng, Y. Li, W. Feng. Poly(N-isopropylacrylamide)-Based Smart Hydrogels: Design, Properties and Applications. *Prog. Mater. Sci*. **2021**, 115, 100702.

[9] Y. J. Kim and Y. T. Matsunaga. Thermo-responsive Polymers, Their Application as Smart Biomaterials. *J. Mater. Chem. B* **2017**, 5, 4307-4321.

[10] M. Karbarz, M. Mackiewicz, K. Kaniewska, K. Marcisz, Z. Stojek. Recent Developments in Design and Functionalization of Micro- and Nanostructural

Environmentally-Sensitive Hydrogels Based on N-Isopropylacrylamide. *Appl. Mater. Today* **2017**, 9, 516-532.

[11] F. D. Jochum, P. Theato. Temperature- and Light-Responsive Smart Polymer Materials. *Chem. Soc. Rev.* **2013**, 42, 7468-7483.

[12] X. Zhang, L. Chen, K.H. Lim, S. Gonuguntla, K. W. Lim, D. Pranantyo, W. P. Yong, W. J. T. Yam, Z. Low, W. J. Teo, H. P. Nien, Q. W. Loh, S. Soh. The Pathway to Intelligence: Using Stimuli-Responsive Materials as Building Blocks for Constructing Smart and Functional Systems. *Adv. Mater.* **2019**, 31, 1804540.

[13] C. Cadart, E. Zlotek-Zlotkiewicz, M. L. Berre, M. Piel, H. K. Matthews. Exploring the Function of Cell Shape and Size During Mitosis. *Dev. Cell* **2014**, 29, 159-169.

[14] S. Ghosh, T. Cai. Controlled actuation of alternating magnetic field-sensitive tunable hydrogels. *J Phys. D: Appl. Phys.* **2010**, 43, 415504.

[15] A. Mamada, T. Tanaka, D. Kungwatchakun, M. Irie. Photoinduced Phase Transition of Gels. *Macromolecules* **1990**, 23, 1517-1519.

[16] T. Satoh, K. Sumaru, T. Takagi, T. Kanamori. Fast-reversible Light-Driven Hydrogels Consisting of Spirobenzopyran-Functionalized Poly(N-isopropylacrylamide). *Soft Matter* **2011**, 7, 8030-8034.

[17] Y. Jin, Y. Shen, J. Yin, J. Qian, Y. Huang. Nanoclay-based self-supporting responsive nanocomposite hydrogels for printing applications. *ACS Appl. Mater. Interfaces* **2018**, 10, 10461-10470.

[18] J. Liu, N. Wang, L. J. Yu, A. Karton, W. Li, W. Zhang, F. Guo, L. Hou, Q. Cheng, L. Jiang, D. A. Weitz, Y. Zhao. Bioinspired graphene membrane with temperature tunable channels for water gating and molecular separation. *Nat. Commun.* **2017**, 8, 2011.

[19] E. Aznar, M. Oroval, L. Pascual, J. R. Murguía, R. M. Máñez, F. Sancenón. Gated Materials for On-Command Release of Guest Molecules. *Chem. Rev.* 2016, 116, 561-718.

[20] Q. Zhao, X. Yang, C. Ma, D. Chen, H. Bai, T. Li, T. Xie. A Bioinspired Reversible Snapping Hydrogel Assembly. *Mater. Horiz.* **2016**, 3, 422-428.

[21] X-H. Li, C. Liu, S-P. Feng, N. X. Fang. Broadband Light Management with Thermochromic Hydrogel Microparticles for Smart Windows. *Joule* **2019**, 3, 290-302.

[22] M. A. Haque, G. Kamita, T. Kurokawa, K. Tsujii, J. P. Gong. Unidirectional Alignment of Lamellar Bilayer in Hydrogel: One-Dimensional Swelling, Anisotropic Modulus, and Stress/Strain Tunable Structural Color. *Adv. Mater.* **2010**, 22, 5110-5114.

[23] K. Mito, M. A. Haque, T. Nakajima, M. Uchiumi, T. Kurokawa, T. Nonoyama, J. P. Gong. Supramolecular Hydrogels with Multi-Cylindrical Lamellar Bilayers: Swelling-Induced Contraction and Anisotropic Molecular Diffusion. *Polymer* **2017**, 128, 373-378.

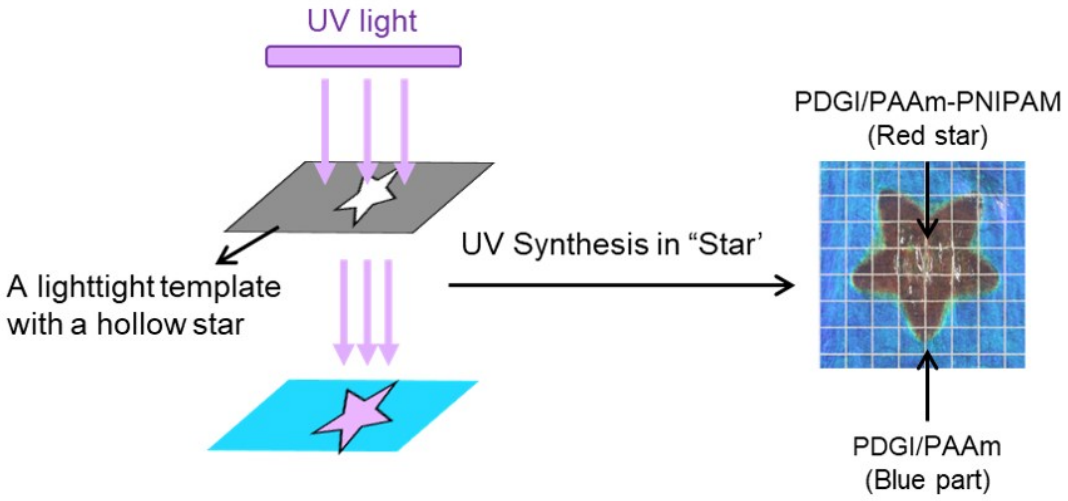

Figure 6-1: Regioselective synthesis of the thermo-responsive PDGI/PAAm-PNIPAM pattern in the PDGI/PAAm hydrogel.

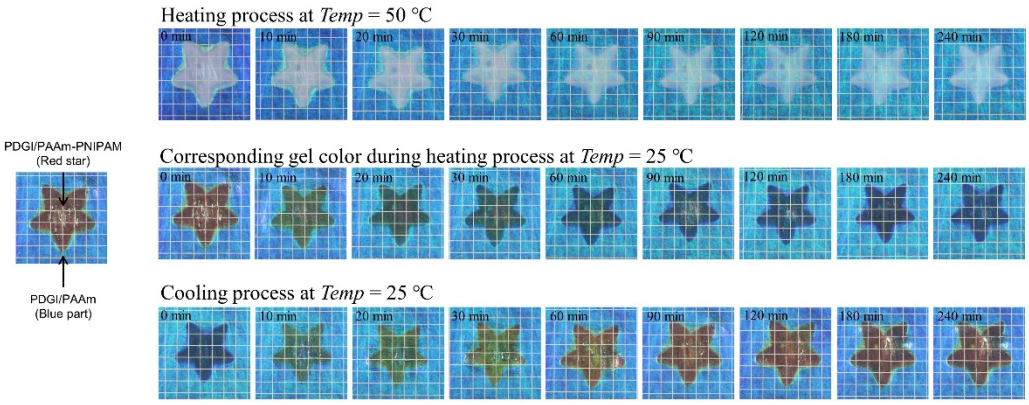

Figure 6-2: The structural color/turbid change of the PDGI/PAAm-PNIPAM gel pattern in the PDGI/PAAm gel upon heating and cooling processes. Background lattices: 5 × 5 mm.

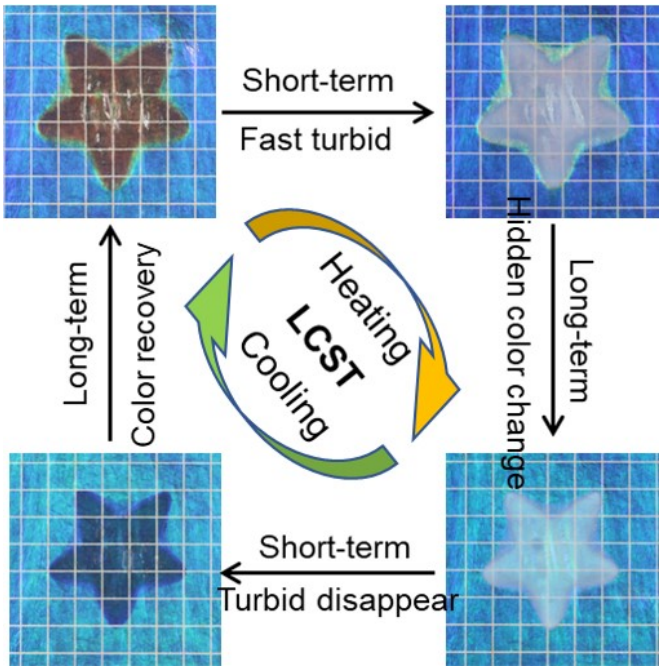

Figure 6-3: The structural color/turbid transition of thermo-responsive PDGI/PAAm-PNIPAM gel pattern in PDGI/PAAm gel during heating and cooling process for applications, such as of smart window and smart display. Background lattices: 5 × 5 mm.

Chapter 7: General Conclusion

In this work, a thermo-responsive photonic PDGI/PAAm-PNIPAM hydrogel with 2-D lamellar structure has been successfully synthesized. PNIPAM was effectively incorporated into the PAAm soft layer of the PDGI/PAAm lamellar gel base, forming an interpenetrating PAAm-PNIPAM layers within the monodomain PDGI bilayers, all while maintaining the anisotropic structure. The gels not only exhibit unique properties, such as reversible deswelling/reswelling behavior due to phase separation behavior near LCST, but also permit tunable structural color, turbidity, and swelling anisotropy by temperature and PNIPAM density. Notably, the gel exhibits ultrafast and reversible structural color/turbid transition around LCST, offering wide range and reversible switching of the stop-band position upon heating and cooling process. The structural color/turbid transition observed in this work represents a unique approach in smart window technology. Moreover, PNIPAM can be regioselectively incorporated into the specific region of the lamellar hydrogels by photomasking during UV polymerization. It is anticipated that this smart PNIPAM-based lamellar photonic hydrogel, with phase separation behavior holds great potential for applications in smart windows, sensors, and smart displays. Conclusions of this dissertation are as follows:

In **Chapter 3**, the strategy towards introducing thermo-responsive PNIPAM polymers into photonic PDGI/PAAm lamellar gels is introduced in detail and the synthetic procedure of PDIG/PAAm-PNIPAM hydrogel is included. The PDGI/PAAm-PNIPAM gels were synthesized by incorporating second networks (PNIPAM) into

PAAm soft layers of PDGI/PAAm lamellar gels. The thermo-induced phase separation behavior of PDGI/PAAm-PNIPAM gel is introduced. Importantly, the PDGI/PAAm-PNIPAM hydrogel shows tunable turbidity and structural color by controlling incorporated PNIPAM concentration. The effect of heating temperature and heating time on the transmittance of the PDGI/PAAm-PNIPAM$_{0.5M}$ gel is also been described in detail. The turbidity of the gel increases with increasing heating temperature above LCST. And the PDGI/PAAm-PNIPAM hydrogels undergo phase separation due to entropy-driven dehydration and collapse upon heating when heating temperature is above the LCST. The transmittance of the gel barely changed with increasing heating time at *Temp* > LCST, which is in associated with LCST-type gels where the turbidity is determined by the heating temperature after reaching equilibrium independent of the heating time.

In **Chapter 4**, the anisotropic lamellar structure of the thermo-responsive lamellar PDGI/PAAm-PNIPAM gel is investigated. After incorporation of thermo-responsive PNIPAM polymers, the photonic PDGI/PAAm hydrogel possesses the thermo-responsibility of PNIPAM around LCST. The deswelling/reswelling behaviors of PDGI/PAAm-PNIPAM gel during heating and cooling processes around LCST is also investigated. The thermo-responsive lamellar hydrogels show structural color/turbid transition during heating and cooling processes. The long-term thermo-responsive behaviors of the PDGI/PAAm-PNIPAM gels is introduced. The gels show long-term structural color tunability and anisotropic deswelling/reswelling behaviors. The turbidity and deswelling/reswelling ratios of the photonic PDGI/PAAm-PNIPAM gels

can be tuned by temperature stimuli, leading the structure color/turbid transition of the gel around LCST.

In **Chapter 5**, the effect of PNIPAM concentration on PDGI/PAAm-PNIPAM gel during heating and cooling process around LCST is introduced in detail, including on turbidity, structural color, interplanar distance, anisotropic swelling, and reversibility. The structural color of PDGI/PAAm-PNIPAM gel can be tuned by controlling NIPAM concentration. Effect of the incorporated PNIPAM concentration on the ultrafast turbidity transition was investigated. High NIPAM concentration hydrogels show low turbidity. High NIPAM concentration gel shows larger shift in color during heating and cooling process. The concentration of incorporated PNIPAM networks significantly influences the extent of deswelling and reswelling. The higher the NIPAM concentration, the greater the extent of the decrease in peak wavelength, λ_{max} and interplanar distance, *d*. This indicates that the NIPAM concentration plays a rule in the variations of λ_{max} and *d* which is in accord with the color shift of the gel. The extent of deswelling/reswelling along diameter direction increases with the NIPAM concentration. On the other hand, swelling anisotropy became less obvious with increasing NIPAM concentration. The gels recovered to the original state upon cooling process, indicating fully reversible color shift independent of the NIPAM concentration.

In **Chapter 6**, the synthesis procedure of pattern PDGI/PAAm-PNIPAM in PDGI/PAAm hydrogel is described in detail. The preparation of PDGI/PAAm-PNIPAM star in PDGI/PAAm gel were introduced. PNIPAM can be regioselectively incorporated into the specific region of the lamellar hydrogels by photomasking during UV

polymerization. The structure color/turbid transition of the PDGI/PAAm-PNIPAM gel pattern in PDGI/PAAm gel during heating and cooling process around LCST is investigated. The applications of the pattern gel are also introduced. The star region immediately turns turbid owing to the thermo-induced phase separation of PNIPAM. Like the normal PDGI/PAAm-PNIPAM hydrogels, the star region in the gel exhibited long-term shrinkage with blue-shift in gel color upon heating and recovery of the structural color upon cooling. This immediate structural color/turbid transition and long-term structural color shift of patterned gel can be used as smart stained glass or smart display.

Accomplishments

Paper related to this dissertation

1. **Yang Han**, Yunzhou Guo, Tasuku Nakajima and Jian Ping Gong. Thermoresponsive Lamellar Hydrogels with Tunable Turbidity, Structural Color, and Anisotropic Swelling. ***ACS Appl. Mater. Interfaces*** **2023**, 15, 49, 57687–57698. https://doi.org/10.1021/acsami.3c14334

Acknowledgements

As I stand on the threshold of completing my doctoral journey, I am deeply grateful for the unwavering support and encouragement I have received from numerous individuals who have played a crucial role in shaping this remarkable chapter of my life.

First and foremost, I extend my heartfelt gratitude to my advisor, Professor Jian Ping Gong, and Professor Tasuku NAKAJIMA. Their exceptional guidance, mentorship, and scholarly insights have been instrumental in honing my research skills and expanding my intellectual horizons. Their unwavering commitment to academic excellence and their passion for advancing scientific knowledge have inspired me every step of the way. In times of challenges, Professor Gong and Professor NAKAJIMA offered patient guidance and constructive feedback that propelled me forward. I am truly indebted to Professor Gong and Professor NAKAJIMA for their profound impact on my academic and personal growth. Their attitude towards research serves as a beacon for my future approach to work, study, and life. Espetially, I am very appreciate their patience and understanding when I wanted to come back to LSW again after the end of the leave of absence from Hokkaido University. Their understanding gives me the courage to continue my doctoral program and to pursuit the thing that I've already given up on but am still unwilling to let go of. During the one year’s leave of absence, I am lack of confidence and courage. Their welcome not just has given me the confidence to continue on the doctoral program, but also the life journey.

I am also deeply appreciative of the kindness and help of all the Professors, staffs, and students in LSW and TSW lab. The kindness and support of the lab members have played a pivotal role in helping my research and life.

Furthermore, my appreciation extends to my family, especially my husband. I am incredibly grateful for my family's care, understanding, and unwavering support.

I also wish to acknowledge the mentors, friends, and peers who have crossed my path during my academic pursuit. Their companionship and shared experiences have enriched my journey beyond measure.

As I conclude this doctoral dissertation, I am acutely aware of the personal growth and intellectual enrichment that have marked my passage through this rigorous process. My heartfelt gratitude goes out to each and every person who has lent their support. Without your guidance and belief in my potential, I would not have achieved what I have today. Please accept my sincerest appreciation and respect.

With deepest gratitude and warmest regards,

HAN, Yang

Laboratory of Soft & Wet Matter

Graduate School of Life Science

Hokkaido University

Sapporo, Japan

Date: [15th November, 2023]